AD-A192 101 SOLVENT DYNAMICAL EFFECTS IN ELECTRON TRANSFER: COMPARISONS OF SELF-EXCHA..(U) PURDUE UNIV LAFAYETTE IN DEPT OF CHEMISTRY R M NIELSON ET AL. 17 FEB 88 TR-77 1/1

UNCLASSIFIED N00014-86-K-0556 F/G 7/2 NL

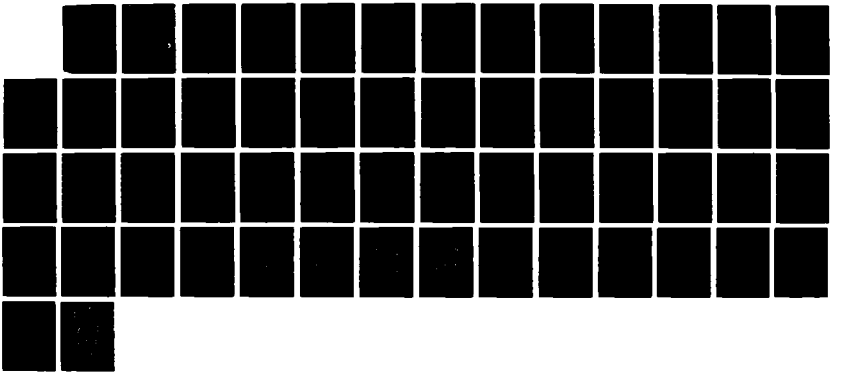

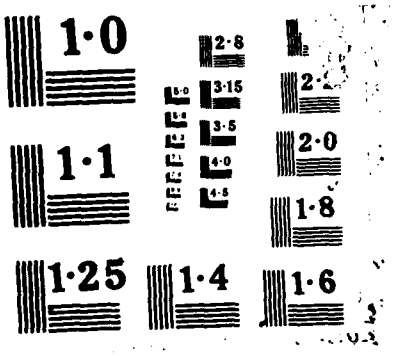
1·0
1·1
1·25
1·4
1·6
2·8
3·15
3·5
4·0
4·5
2·0
1·8

OFFICE OF NAVAL RESEARCH

Contract N00014-86-K-0556

Technical Report No. 77

Solvent Dynamical Effects in Electron Transfer: Comparisons of Self-Exchange Kinetics for Cobaltocenium-Cobaltocene and Related Redox Couples with Theoretical Predictions

by

R. M. Nielson, G. E. McManis, M. N. Golovin, and M. J. Weaver

Prepared for Publication

in the

Journal of Physical Chemistry

Purdue University

Department of Chemistry

West Lafayette, Indiana 47907

February 17, 1988

SECURITY CLASSIFICATION OF THIS PAGE

REPORT DOCUMENTATION PAGE

1a REPORT SECURITY CLASSIFICATION Unclassified	1b RESTRICTIVE MARKINGS
2a SECURITY CLASSIFICATION AUTHORITY	3 DISTRIBUTION / AVAILABILITY OF REPORT Approved for public release and sale; its distribution is unlimited.
2b DECLASSIFICATION / DOWNGRADING SCHEDULE	
4 PERFORMING ORGANIZATION REPORT NUMBER(S) Technical Report No. 77	5 MONITORING ORGANIZATION REPORT NUMBER(S)
6a NAME OF PERFORMING ORGANIZATION Purdue University Department of Chemistry 6b OFFICE SYMBOL (If applicable)	7a NAME OF MONITORING ORGANIZATION Division of Sponsored Programs Purdue Research Foundation
6c ADDRESS (City, State, and ZIP Code) Purdue University Department of Chemistry West Lafayette, IN 47907	7b ADDRESS (City, State, and ZIP Code) Purdue University West Lafayette, IN 47907
8a NAME OF FUNDING / SPONSORING ORGANIZATION Office of Naval Research 8b OFFICE SYMBOL (If applicable)	9 PROCUREMENT INSTRUMENT IDENTIFICATION NUMBER
8c ADDRESS (City, State, and ZIP Code) 800 N. Quincy Street Arlington, VA 22217	10 SOURCE OF FUNDING NUMBERS PROGRAM ELEMENT NO / PROJECT NO / TASK NO / WORK UNIT ACCESSION NO

11 TITLE (Include Security Classification)
Solvent Dynamical Effects in Electron Transfer: Comparisons of Self-Exchange Kinetics for Cobaltocenium-Cobaltocene and Related Redox Couples with Theoretical Predictions

12 PERSONAL AUTHOR(S)
R. M. Nielson, G. E. McManis, M. N. Golovin, and M. J. Weaver

13a TYPE OF REPORT	13b TIME COVERED	14 DATE OF REPORT (Year, Month, Day)	15 PAGE COUNT
Technical	FROM _____ TO _____	February 17, 1988	

16 SUPPLEMENTARY NOTATION

17 COSATI CODES			18 SUBJECT TERMS (Continue on reverse if necessary and identify by block number)
FIELD	GROUP	SUB-GROUP	self-exchange kinetics, solvent-dynamical effects, cobaltocenium-cobaltocene redox couples, nmr line broadening

19 ABSTRACT (Continue on reverse if necessary and identify by block number)

Rate constants, k_{ex}, and activation parameters for the self exchange of cobaltocenium-cobaltocene, $Cp_2Co^{+/o}$, and the decamethyl derivative, $Cp_2^*Co^{+/o}$, in thirteen organic solvents have been evaluated using the proton nmr line-broadening technique with the objective of probing the influence of solvent dynamics upon the electron-transfer kinetics. Together with some corresponding measurements reported earlier for ferrocenium-ferrocene, $Cp_2Fe^{+/o}$, additional measurements for the decamethyl derivative, $Cp_2^*Fe^{+/o}$, and with corresponding data for $Cp_2Co^{+/o}$ electrochemical exchange, these results enable a systematic comparative examination to be made of the effects of solvent dielectric relaxation on the barrier-crossing frequency for such simple outer-sphere reactions. For the facile $Cp_2Co^{+/o}$ couple, the solvent dependence of the "observed" frequency factors, $\nu_n(ob)$, extracted from the k_{ex} values by correcting for the solvent-dependent barrier height, ΔG^*, is in approximate accordance with the relative frequency factors, $\nu_{os}(calc)$, predicted from the continuum model of overdamped solvent relaxation. The sub-unity (ca. 0.7-0.8)
(continued on back)

20 DISTRIBUTION / AVAILABILITY OF ABSTRACT	21 ABSTRACT SECURITY CLASSIFICATION
☐ UNCLASSIFIED/UNLIMITED ☒ SAME AS RPT ☐ DTIC USERS	Unclassified
22a NAME OF RESPONSIBLE INDIVIDUAL	22b TELEPHONE (Include Area Code) / 22c OFFICE SYMBOL

DD FORM 1473, 84 MAR — 83 APR edition may be used until exhausted. All other editions are obsolete.

SECURITY CLASSIFICATION OF THIS PAGE

ABSTRACT

Rate constants, k_{ex}, and activation parameters for the self exchange of cobaltocenium-cobaltocene, $Cp_2Co^{+/o}$, and the decamethyl derivative, $Cp_2'Co^{+/o}$, in thirteen organic solvents have been evaluated using the proton nmr line-broadening technique with the objective of probing the influence of solvent dynamics upon the electron-transfer kinetics. Together with some corresponding measurements reported earlier for ferrocenium-ferrocene, $Cp_2Fe^{+/o}$, additional measurements for the decamethyl derivative, $Cp_2'Fe^{+/o}$, and with corresponding data for $Cp_2Co^{+/o}$ electrochemical exchange, these results enable a systematic comparative examination to be made of the effects of solvent dielectric relaxation on the barrier-crossing frequency for such simple outer-sphere reactions. For the facile $Cp_2'Co^{+/o}$ couple, the solvent dependence of the "observed" frequency factors, $\nu_n(ob)$, extracted from the k_{ex} values by correcting for the solvent-dependent barrier height, ΔG^*, is in approximate accordance with the relative frequency factors, $\nu_{os}(calc)$, predicted from the continuum model of overdamped solvent relaxation. The su unity (ca. 0.7-0.8) slope of the logarithmic $\nu_n(ob)$ - $\nu_{os}(calc)$ plot for $Cp_2'Co^{+/o}$ self exchange is consistent with a recent theoretical prediction of the combined effect of overdamped solvent motion and reactant vibrations (ref. 2g). In a given solvent, the sequence of k_{ex} values is $Cp_2'Co^{+/o} > Cp_2Co^{+/o} \simeq Cp_2'Fe^{+/o} > Cp_2Fe^{+/o}$, with $Cp_2Co^{+/o}$ and $Cp_2Fe^{+/o}$ being about 10- and 100-fold slower, respectively, than $Cp_2'Co^{+/o}$ self exchange. While these reactivity differences can be traced to variations in donor-acceptor orbital overlap, the solvent dependencies of k_{ex} for $Cp_2Co^{+/o}$ and $Cp_2Fe^{+/o}$ electron exchange nevertheless exhibit a strong influence from overdamped solvent relaxation. Marked deviations from the dielectric continuum predictions are seen, however, in several solvents. Thus the barrier-crossing frequencies in propylene carbonate, N-methylformamide, and especially methanol are substantially (4-100 fold) larger than expected from $\nu_{os}(calc)$, implicating the presence of surprisingly rapid relaxation modes in these solvents. The solvent-dependent activation parameters also differ significantly from the expectations of conventional theoretical models.

We have recently been studying in detail the solvent-dependent electrochemical exchange kinetics of metallocene and related redox couples,[1] with the overall objective of examining the influence of solvent reorganization dynamics upon the rate parameters in relation to recent theoretical predictions for electron-transfer processes.[2] Metallocene couples have several important attributes for this purpose, including known small inner-shell (i.e. reactant bond distortional) barriers, small or negligible work-term effects upon the measured rate constants,[3] and exhibit chemical reversibility in a variety of nonaqueous media. The observed kinetics in a range of solvents at mercury electrodes provide clear evidence for the presence of a solvent-dependent preexponential factor.[1] The observed behavior is roughly consistent with the predictions of a dielectric continuum dynamical model in the "overdamped" limit,[1a,b] although alcohol solvents exhibit striking deviations from this pattern.[1c] Roughly comparable findings have been reported for several other electron exchange systems, involving organic redox couples, at electrodes and in homogeneous solution.[4]

Reported here is a detailed examination of rate constants and activation parameters for the homogeneous-phase self-exchange of cobalticenium-cobaltocene, $Cp_2Co^{+/o}$ (Cp - cyclopentadienyl) and its decamethyl derivative, $Cp'_2Co^{+/o}$ (Cp' - pentamethyl-cyclopentadienyl), in thirteen solvents using the proton nmr line-broadening technique. The objectives are several. Firstly, since our most extensive measurements of rate constants for electrochemical exchange are for the $Cp_2Co^{+/o}$ couple,[1c] it is clearly of interest to ascertain if similar behavior is obtained for the corresponding reactions in homogeneous solution.

Secondly, when this study was underway it became apparent that the $Cp_2Co^{+/o}$ couple exhibits markedly different self-exchange kinetics to those for the ferrocenium-ferrocene couple, $Cp_2Fe^{+/o}$, the latter reported previously by Wahl and coworkers.[5] Further examination of $Cp_2Co^{+/o}$ in comparison with $Cp_2Fe^{+/o}$ and the corresponding decamethyl couples $Cp_2'Co^{+/o}$ and $Cp_2'Fe^{+/o}$ revealed the presence of large systematic differences in the self-exchange rate constants, k_{ex}.[6] The sequence of k_{ex} values in a given solvent is $Cp_2Fe^{+/o} < Cp_2'Fe^{+/o} \approx Cp_2Co^{+/o} < Cp_2'Co^{+/o}$, the rate constants for $Cp_2'Co^{+/o}$ being around 10 and 100 fold larger than for $Cp_2Co^{+/o}$ and $Cp_2Fe^{+/o}$, respectively. These rate variations are entirely unexpected on the basis of nuclear rearrangement factors, and appear to be due to differences in the extent of electronic coupling between the donor and acceptor orbitals.[6] In harmony with this interpretation, substantially stronger electronic coupling is deduced for intervalence charge transfer in bicobaltocene with respect to corresponding biferrocene cations.[7] This marked reactivity dependence upon reactant electronic structure is apparently absent for the corresponding electrochemical exchange processes.[1b]

It is therefore of interest to ascertain if the nature and extent of the solvent dynamical contribution to the observed kinetics, as exposed by the form of the rate-solvent dependence, may also depend on the metallocene structure and/or reaction environment. This might be anticipated since the degree to which the preexponential factor is controlled by overdamped solvent motion can be determined by the degree of donor-acceptor electronic coupling[2c,8] as well as the relative contributions of inner-shell and solvent reorganization to the free-energy barrier.[2f,g]

Of central concern here, therefore, is a comparative examination of the solvent-dependent exchange kinetics for these reactant systems in relation to the predictions of theoretical electron-transfer models. While the observed reactivity trends provide further evidence supporting the importance of overdamped solvent motion to the barrier-crossing frequency, they also uncover some significant and surprising deviations from the predicted behavior.

EXPERIMENTAL

Material and Sample Preparation. Ferrocene (Cp_2Fe), decamethylferrocene ($Cp_2'Fe$), and cobaltocene (Cp_2Co) were obtained from Strem Chemicals. Cobaltocenium tetrafluoroborate ($Cp_2Co\ BF_4$) was prepared via oxidation of Cp_2Co with tetrafluoroboric acid (Alfa). Ferrocenium tetrafluoroborate ($Cp_2Fe\ BF_4$) was prepared by oxidizing Cp_2Fe and $Cp_2'Fe$, respectively, with nitrosonium tetrafluoroborate (Lancaster Synthesis, Ltd.) in dichloromethane. Decamethylcobaltocene ($Cp_2'Co$) and decamethylcobaltocenium hexafluorophosphate ($Cp_2'Co\ PF_6$) were prepared as described in ref. 9. The solvents were high-purity grades from Burdick and Jackson, Aldrich, or Fluka were purified further using standard procedures.[10]

All solutions for nmr examination were prepared within a dry-nitrogen glove box and placed in 5 mm nmr tubes, which were then flame sealed on a vacuum line. Samples prepared in this manner were stable for several days. The concentrations of the diamagnetic-paramagnetic species were: Cp_2CoBF_4, 0.02-0.12 M (typically 0.04 M); Cp_2Co, 0.7-20 mM (typically 0.01 M); $Cp_2'CoPF_6$, 0.02-0.025 M; $Cp_2'Co$, 0.8-8 mM; $Cp_2'Fe$, ca. 0.025 M; $Cp_2'FeBF_4$, ca. 5 mM; Cp_2Fe, 0.08 M; Cp_2FeBF_4, 1 mM. The solutions usually contained 0.10

M tetraethylammonium tetrafluoroborate (Et_4NBF_4) as inert electrolyte, and 1% tetramethylsilane as a chemical shift reference.

NMR Data Collection and Analysis. Proton nmr spectra were collected on Nicolet NT200 and NT470 instruments operating at 200.0 and 469.6 MHz, respectively. Data acquisition utilized a single-pulse technique with a 5 to 9 μs pulse width. The acquired block size was 16 or 32 K. In proteated media, the solvent peak(s) was suppressed by homonuclear irradiation of the undesirable resonance(s) using a minimum of radio-frequency power to avoid significant dielectric heating. Since no deuterium was present for many of the samples, no field/frequency lock was used. Spectra collected under these conditions had excellent signal-to-noise ratios after approx. 100 scans. The temperature was controlled with a gas-flow device and measured with a substitution technique using methanol and ethylene glycol standard samples;[11] it was stable to $\pm$ 0.5°C and reproducible to $\pm$ 1°C.

Peak widths were determined by fitting the data to a Lorentzian line shape using the least-squares-minimizing program available on the Nicolet instruments. In mixtures of diamagnetic and paramagnetic metallocenes, the proton nmr chemical shifts were observed to be the weighted averages of those of the pure metallocenes measured individually, indicating that the electron-transfer process is in the "fast-exchange" region. In these circumstances, the rate constant for electron exchange can be determined from[5]

$$k_{ex} = \frac{4\pi x_D x_P (\Delta\nu)^2}{(W_{DP} - x_P W_P - x_D W_D) C_{tot}} \qquad (1)$$

Here x_D and x_P are the mole fractions of diamagnetic and paramagnetic

species, respectively, $\Delta\nu$ is the difference in resonance frequency (Hz) between the pure diamagnetic and paramagnetic samples, W_{DP}, W_P, and W_D are the nmr line widths (Hz) at half height for the mixed, pure paramagnetic, and pure diamagnetic samples, respectively, and C_{tot} is the total molar concentrations of the diamagnetic and paramagnetic species. In practice, x_P could be determined most accurately from the chemical shift data themselves using

$$x_P = \frac{\nu_{DP} - \nu_D}{\Delta\nu} \qquad (2)$$

where the subscripts are as before and ν is the resonance frequency. Therefore, to obtain a single rate constant, the chemical shifts and line widths of three samples are needed: those for the pure diamagnetic, the pure paramagnetic, and the diamagnetic-paramagnetic mixture.

The true line widths of the samples containing pure $Cp_2'Co$ could not be measured directly due to the presence of ca. 1% diamagnetic $Cp_2'Co^+$ impurity. To obtain W_P, several acetone solutions were made with constant x_D and x_P but varying C_{tot}, and the resulting line widths plotted versus $1/C_{tot}$. This gave a straight line with an intercept of $(x_DW_D + x_PW_P)$, enabling W_P to be obtained. Values of W_P for other solvents were estimated from the relative solvent viscosities. Such a procedure predicts W_P for $Cp_2'Co$ in pentane to be 40 Hz, which compares favorably to the measured value of 35 Hz ($Cp_2'Co^+$ is insoluble in pentane which permits the direct measurement of W_p). Fortunately, precise values of W_P were not necessary since the contribution of the paramagnetic species to the total line width was always less than 8%, i.e. the dominant contribution to W_{DP} arises from electron exchange. However, due to the tedium associated with this

procedure, systematic measurements of k_{ex} for $Cp_2'Co^{+/o}$ as a function of temperature were not undertaken.

Values of these and related experimental nmr parameters for the systems considered here are summarized in the Supplementary Material.

RESULTS AND THEORETICAL ANALYSES

Solvent-Dependent Rate Constants

Table I contains a summary of rate constants, k_{ex}, for the self exchange of $Cp_2Co^{+/o}$ in thirteen nonaqueous solvents at 25°C. The selection of these media was based on several factors. As for our earlier electrochemical kinetic studies,[1] it is desirable to select solvents that span a wide range of documented dynamical as well as dielectric behavior. The media selected here (Table I) overlap considerably with those examined in ref. 1, including the simple aprotic solvents acetonitrile, benzonitrile, acetone, dichloromethane (CH_2Cl_2), the amides N,N-dimethylformamide (DMF), N-methylformamide (NMF), tetramethylurea (TMU), and also dimethylsulfoxide (DMSO), propylene carbonate (PC), and methanol. The last solvent is of interest in view of the observed marked deviations of the $Cp_2Co^{+/o}$ electrochemical exchange and $Cp_2Fe^{+/o}$ self-exchange kinetics from simple theoretical expectations in this medium.[1c] The other solvents examined here, 1,2-dichloroethane [$(CH_2Cl)_2$], pyridine, and hexamethylphosphoramide (HMPA) were selected to further increase the range of relaxation times encountered. Six of these solvents have also been employed in an earlier detailed examination of $Cp_2Fe^{+/o}$ and $Cp_2'Fe^{+/o}$ self exchange by Wahl et al.[5a]

Practical considerations provide a substantial limitation on the range

of media for which k_{ex} values can be obtained for the present systems using proton nmr. Firstly, the solubility of $Cp_2Co \cdot BF_4$ and especially $Cp_2'Co \cdot PF_6$ was often found to be insufficient to yield satisfactory spectra. Secondly, most of the solvents were unavailable in the deuterated form. Although solvent peak suppression was employed (vide supra), this tactic was difficult or even impractical for examining systems where the reactant and solvent proton peaks overlapped considerably.

Nevertheless, data could be obtained in a sufficiently large range of solvents (Table I), especially for $Cp_2Co^{+/o}$, so to enable systematic comparisons to be made, both with our earlier electrochemical exchange data[1] and those for $Cp_2Fe^{+/o}$ and $Cp_2'Fe^{+/o}$ self exchange.[5] Data for the latter two reactions are also included in Table I; besides k_{ex} values taken from ref. 5, we include values obtained in the present study for $Cp_2'Fe^{+/o}$ in benzonitrile and pyridine. Based on the standard deviations from replicate measurements, the k_{ex} values are adjudged to be precise to within ca. 10%. In some cases, k_{ex} values were obtained in coresponding deuterated and proteated solvents (e.g. $Cp_2Co^{+/o}$ in CH_3OH and CH_3OD); the values generally agreed to within 10%. As noted above, most k_{ex} measurements for $Cp_2Co^{+/o}$ and $Cp_2'Co^{+/o}$ employed ca. 0.04 M cobalticenium ions together with 0.1 M Et_4NBF_4; the data summarized for these reactions in Table I refer to this condition. Measurements of $Cp_2Co^{+/o}$ self exchange in acetonitrile, acetone, and methanol indicate that k_{ex} depends mildly yet significantly on the supporting electrolyte concentration; thus for $[Et_4NBF_4]$ = 0, 0.1 M, and 0.5 M in acetonitrile, k_{ex} = 4.5, 3.8, and 3.25 x 10^7 M^{-1} s^{-1}, respectively. Slightly larger electrolyte effects were observed for $Cp_2Co^{+/o}$ in dichloromethane. These decreases in k_{ex} with increasing ionic strength are comparable to those reported for $Cp_2Fe^{+/o}$ in

acetonitrile.[5] Since most k_{ex} data for $Cp_2Fe^{+/o}$ and $Cp_2'Fe^{+/o}$ reported in ref. 5 were obtained in the absence of added electrolyte, all the k_{ex} values given for these two reactions in Table I refer to this condition.

As in our earlier studies,[1] it is of central interest to compare these solvent-dependent rate constants with the corresponding theoretical predictions. A convenient formalism for this purpose is given by[19]

$$k_{ex} = K_p \kappa_{el} \nu_n \exp\left[-(\Delta G^*_{os} + \Delta G^*_{is})/RT\right] \quad (3)$$

where K_p is an equilibrium constant for forming the precursur state from the separated reactants, ν_n is the nuclear frequency factor, κ_{el} is the electronic transmission coefficient, and ΔG^*_{os} and ΔG^*_{is} are the outer- and inner-shell components, respectively, of the intrinsic free energy of activation (i.e. that associated with solvent and reactant reorganization).

Of primary concern here is the manner and extent to which the preexponential factor in Eq. (3), presumably the nuclear component ν_n, is dependent on the solvent. However, in order to utilize solvent-dependent k_{ex} values for this purpose, it is clearly necessary to correct them for variations in the activation energy. The inner-shell component, ΔG^*_{is}, should be essentially solvent independent and is small for the present systems. [The ΔG^*_{is} values for $Cp_2Co^{+/o}$ and $Cp_2Fe^{+/o}$ are estimated from crystallographic and Raman spectroscopic data to be about 0.7 and 0.35 kcal mol^{-1}, respectively, with comparable (or slightly smaller) values for the decamethyl analogs.[6]]

However, ΔG^*_{os} is expected to be solvent dependent so to partially mask the contribution from the preexponential component.[1b,c] The simplest approach is to calculate ΔG^*_{os} from the dielectric continuum model, which for a pair of equal-sized spherical reactants takes the form[20]

$$\Delta G^{*}_{os} = (e^2/4)(a^{-1} - R^{-1})(\epsilon_{op}^{-1} - \epsilon_{s}^{-1}) \quad (4)$$

where e is the electronic charge, a is the reactant radius, R is the internuclear distance in the precursor state, and ϵ_{op} and ϵ_s are the optical and static dielectric constants, respectively. For the present metallocenes we take, as before,[1] an effective radius of 3.8 Å, and assume that the reactants are in contact, so that 2a = R [Possible errors in this "scaling factor" in Eq. (4) are discussed below]. For simplicity, we assume that the radius of the decamethyl derivatives are the same as for $Cp_2Co^{+/o}$ and $Cp_2Fe^{+/o}$, although in actuality the former may be slightly larger, leading to correspondingly smaller ΔG^{*}_{os} values (vide infra). The resulting estimates of ΔG^{*}_{os} are listed for each solvent in Table II. The ϵ_{op} and ϵ_s values used for this purpose were taken from the compilation in Table II of ref. 1c, and also from Table III in the present paper; the latter contains relevant properties of solvents that were not considered in ref. 1c.

Although not essential, it is convenient also to provide an estimate for $K_p\kappa_{el}$ so that absolute values of ν_n can be extracted from the experimental k_{ex} values. For simplicity, we initially take $\kappa_{el} = 1$ (i.e. the reaction pathway is assumed to be adiabatic at least at the reactants' closest approach). Again following ref. 1b, we initially estimate K_p from (vide infra)[19]

$$K_p = 4\pi N r^2 \delta r \quad (5)$$

where N is Avogadro's number, r is the closest internuclear separation, and δr is the "reaction zone thickness", i.e. the range of additional internuclear separations that feature sufficient donor-acceptor orbital overlap so to contribute importantly to the reaction rate. Taking

$r = 7.6$ Å, and $\delta r = 0.6$ Å,[21] we obtain $K_p = 0.26$ M^{-1}. For each of the present systems, then, "observed" estimates of ν_n, $\nu_n(ob)$, were obtained from the experimental k_{ex} values by using [cf. Eq. (3)]:

$$\nu_n(ob) = k_{ex}(K_p \exp [-(\Delta G^*_{os} + \Delta G^*_{is})/RT])^{-1} \quad (6)$$

with K_p taken as 0.26 M^{-1}, ΔG^*_{is} as 0.5 kcal mol^{-1} (an average value, vide supra), and the ΔG^*_{os} values from Table II.

It is of interest to compare these solvent-dependent $\nu_n(ob)$ values with those calculated from solvent dynamical models. We will assume initially that ν_n is controlled entirely by the effective nuclear barrier-crossing frequency due to outer-shell (i.e. solvent) motion, ν_{os} (vide infra). A simple relation that enables ν_{os} values for electron-exchange processes to be calculated on the basis of the dielectric continuum treatment, utilizing dielectric loss data,[1,2a-c] is

$$\nu_{os}(calc) = \tau_L^{-1} (\Delta G^*_{os}/4\pi k_B T)^{1/2} \quad (7)$$

where k_B is the Boltzmann constant and τ_L is the so-called longitudinal solvent relaxation time. The latter can be extracted from experimental values of the Debye relaxation time, τ_D, by using[23]

$$\tau_L \simeq (\epsilon_\infty/\epsilon_s)\, \tau_D \quad (7a)$$

where ϵ_∞ is the high ("infinite") frequency dielectric constant. (It is important to note that the τ_L values are substantially smaller than τ_D, reflecting the acceleration of the dielectric relaxation brought about by interaction with surrounding solvent dipoles.[23]) Values of $\nu_{os}(calc)$ for each solvent calculated from Eqs. (7) and (7a) are listed in Table II,

along with the corresponding τ_L values. The dielectric loss data used to obtain the latter parameter are given in Table III and in Table II of ref. 1c.

As noted previously (e.g. refs. 1b,c,2a), the theoretical treatment leading to Eq. (6) treats the solvent polarization dynamics as being "overdamped", where the motion along the reaction coordinate associated with dipole reorientation is impeded by dielectric friction from surrounding solvent molecules. Most of the solvents considered here probably lie within the overdamped region, although those having the smallest τ_L values (say $\lesssim 0.5$ ps), such as acetonitrile and acetone, approach the "solvent inertial" limit where ν_{os} will be determined partly by the individual solvent rotational time, τ_{rot}.[2a,24] Another assumption made in deriving Eq. (6) is that the barrier top forms a cusp, corresponding to a very small electronic coupling element, H_{12}, between the donor and acceptor orbitals. Consequently, Eq. (6) will overestimate ν_{os} for typical weakly adiabatic reactions (for which one expects that $H_{12} \sim 0.01$ eV[22]), although this error is unlikely to be substantial ($\lesssim$ factor of two).[8]

Comparisons between the ν_n(ob) values obtained from k_{ex} using Eq. (6) in various solvents plotted logarithmically against the corresponding ν_{os} values calculated from Eq. (7), labelled ν_{os}(calc), for $Cp_2Co^{+/o}$ and $Cp'_2Co^{+/o}$ self exchange are shown (filled symbols) in Figs. 1 and 2, respectively. Corresponding data for $Cp_2Fe^{+/o}$ and $Cp'_2Fe^{+/o}$ self exchange are plotted as circles and triangles, respectively, in Fig. 3. The unit slope straight line shown in each case corresponds to ν_n(ob) = ν_{ob}(calc). Also plotted on Fig. 1 (as crosses) are the ν_n(ob) values obtained from the

corresponding rate constants for $Cp_2Co^{+/o}$ *electrochemical* exchange, k_{ex}^{e}, determined at the mercury-solvent interface and reported in ref. 1c. These quantities are obtained by inserting k_{ex}^{e} values in Eq. (6), and employing the estimates of K_p, ΔG_{is}^{*}, and ΔG_{os}^{*} derived using the same physical models as for the homogeneous-phase case but appropriate instead for the heterogeneous reaction geometry. Thus K_p was taken as 6×10^{-9} cm, ΔG_{is}^{*} as 0.25 kcal mol^{-1} (i.e. one half of the self-exchange case), whereas the ΔG_{os}^{*} values are assumed to equal those for the corresponding self-exchange reaction (see footnote 25 and ref. 1c for further explanation and details).

An alternative means of comparing the experimental rate constants involves calculating k_{ex} values from Eq. (3) by taking ν_n to equal the ν_{os}(calc) values from Eq. (7) and inserting the estimates of the other parameters as before. These k_{ex}(calc) values are listed in Table II. [Values of k_{ex}(calc) obtained by using a fixed (i.e. solvent independent) frequency factor, $\nu_n = 1 \times 10^{13}$ s^{-1}, labelled k_{ex}^{f}(calc), are also listed for comparison in Table II.] Given the substantial uncertainties in calculating such absolute k_{ex} values, it is more useful to compare the relative k_{ex} values as the solvent is altered. To this end, ratios of k_{ex}(calc) in a given solvent to that in acetonitrile, $(k_{ex}/k_{ex}^{ACN})_{calc}$, are listed in the far right-hand column in Table I, for comparison with the corresponding experimental rate ratios, k_{ex}/k_{ex}^{ACN}, given for each system in the adjacent columns.

Comparison between these calculated and experimental rate ratios shows that the continuum dynamical model, as embodied in Eq. (7), is able to at least roughly account for the latter values. This is particularly true for the $Cp_2'Co^{+/o}$ reaction for which the calculated and experimental rate ratios

are within twofold of each other in every solvent examined except propylene carbonate. However, the experimental rate ratios, as well as the k_{ex} values themselves (vide supra), are seen to depend significantly on the metallocene structure (Table I).

These general trends may also be gleaned by inspecting Figs. 1-3. For $Cp_2'Co^{+/o}$ (Fig. 2), the plot displays a remarkably good correlation between ν_n(ob) and ν_{os}(calc), except for propylene carbonate, even though the latter values are systematically (ca. 20 fold) larger. The corresponding relationships obtained for the other three, slower, self-exchange processes (Figs. 1, 3) are less clearcut. Although a rough correlation between ν_n(ob) and ν_{os}(calc) is observed in each case, there are some substantial deviations (vide infra). The lack of such deviations from $Cp_2'Co^{+/o}$ is probably due in part to the more restricted range of solvents for which data could be obtained for this couple relative to $Cp_2Co^{+/o}$.

Alternative Estimates of the Solvent-Dependent Barrier Height

Given the sensitivity of the above solvent-dependent rate analysis to the magnitude of the outer-shell barrier, it is desirable to examine carefully the likely consequences of uncertainties in ΔG^*_{os} on the present analysis, along with alternative methods for estimating this parameter. Direct evidence supporting the approximate validity of the solvent-dependent $(\epsilon_{op}^{-1} - \epsilon_s^{-1})$ functional form of the dielectric continuum expression [Eq. (4)] is available from measurements of optically induced electron transfer within mixed-valence complexes.[26] These measurements have the virtue of enabling the magnitude of the solvent-dependent intrinsic barrier to be estimated from the observed transition energies, E_{op}.[26] Although significant deviations from the expected linearity between

E_{op} and $(\epsilon_{op}^{-1} - \epsilon_s^{-1})$ have been observed,[27] reasonable concordance with this relationship has been obtained not only for several well-studied Ru(III)/(II) dimers[26,27] but also for mixed-valence biferrocene and biferrocenylacetylene cations.[28] The latter two systems are of particular interest here in view of their structural similarity to the precursor complexes for the present self-exchange reactions.

It is therefore worthwhile to examine the effects of estimating $\nu_n(ob)$ values from Eq. (6) by utilizing ΔG_{os}^* values estimated from experimental E_{op} data rather than calculating them from the dielectric continuum expression, Eq. (4). Although such E_{op} values for the mixed-valence biferrocenes are available for several solvents of interest here,[28] acquisition of a more complete data set is precluded by difficulties from insufficient solubility, solute decomposition, etc.[28b] Nevertheless, values of $\nu_n(ob)$ obtained in this manner for $Cp_2Fe^{+/o}$ self exchange (open squares) are plotted against $\nu_{os}(calc)$, obtained as before, in Fig. 4. The required ΔG^* values were obtained from the corresponding observed E_{op} energies for the mixed-valence biferrocenylacetylene cation[28] by assuming, as usual,[26] that $\Delta G^* = E_{op}/4$. (Note that this quantity will contain both ΔG_{is}^* and ΔG_{os}^* components.) The corresponding results obtained using ΔG_{os}^* estimates from Eq. (4) (as in Figs. 1 and 3) are also shown, for $Cp_2Co^{+/o}$ and $Cp_2Fe^{+/o}$ self exchange, as the filled squares in Fig. 4.

Since the E_{op} data yield ΔG^* values (after correction for the ΔG_{is}^* component) that are significantly (0.2-0.8 kcal mol^{-1}) smaller than those from Eq. (4), the former $\nu_n(ob)$ estimates are uniformly smaller than the latter (Fig. 4). Due in part to the limited number of solvents for which the E_{op} data are available and the large scatter in the $\nu_n(ob) - \nu_{os}(calc)$

plots, no clear conclusion can be derived from Fig. 4, although the use of the optical data acts to diminish slightly the degree of dependence of ν_n(ob) upon ν_{os}(calc). Somewhat smaller ΔG^* values are obtained using the E_{op} data for the biferrocene cation, as expected since the Fe-Fe distance is smaller than for the acetylenic-bridged binuclear complex.[28a] Nevertheless, the form of the ν_n(ob) - ν_{os}(calc) plots is not greatly altered if these former ΔG^* estimates are employed instead. The acetylenic derivative, however, is considered more appropriate for the present purpose since the Fe-Fe distance should match closely the likely precursor complex geometries for intermolecular electron transfer.

An alternative to the dielectric continuum model for estimating ΔG^* is provided by a recent treatment employing the mean spherical approximation (MSA) for the solvent.[29] While the absolute values of ΔG^* obtained by this means tend to be ca. 15-25% larger than the dielectric continuum estimates, the functional dependence on the solvent turns out not to differ greatly, at least for the systems considered here. This matter will be taken up in detail elsewhere, with regard to comparisons of E_{op} data with these alternative theoretical models.[28b]

Another line of evidence suggests that while the $(\epsilon_{op}^{-1} - \epsilon_s^{-1})$ term in Eq. (4) provides an approximately correct function describing the solvent dependence of ΔG^*_{os}, the effective "scaling factor" may be significantly smaller than estimated by the $(a^{-1} - R^{-1})$ term. This is obtained by inspecting the ν_n(ob) - ν_{os}(calc) plot for $Cp_2'Co^{+/o}$ self exchange in Fig. 2. While the ν_n(ob) values correlate almost linearly with ν_{os}(calc), the former are 10-20 fold larger than the latter. If the ΔG^*_{os} values [from Eq. (4)] employed to evaluate ν_n(ob) are indeed appropriate, then provided

that the ν_{os}(calc) estimates are approximately correct it follows that the actual K_p values are uniformly 10-20 fold larger than the estimate, 0.26 M^{-1}, employed to obtain ν_n(ob). On the basis of Eq. (5), this would imply that $\delta r \sim$ 5-10 Å. However, such a situation is extremely unlikely since it would imply that the reaction remains adiabatic (i.e. $\kappa_{el} \sim 1$) even for reactant internuclear separations as large as 15 Å. The available evidence strongly suggests that adiabatic outer-sphere pathways are usually restricted to much smaller distances, ca. 5 Å,[22] inferring that $\delta r \sim 1$ Å.

Most likely, then, the observed systematic deviations between ν_n(ob) and ν_{os}(calc) in Fig. 2 reflect the use of ΔG^*_{os} estimates for the former that are systematically too large. In order to test the consequences of this possibility, alternative estimates of ν_n(ob) for $Cp'_2Co^{+/o}$ self exchange were obtained as follows. The ΔG^*_{os} estimate for acetonitrile (a convenient "reference" solvent) was adjusted to a value, 4.25 kcal mol^{-1}, so to yield agreement with ν_{os}(calc) for this system; the ν_n(ob) values for the remaining solvents were then recalculated using ΔG^*_{os} values that were adjusted from the corresponding Eq. (4) values (Table II) by the same proportionality factor (0.74). The resulting ν_n(ob) values are plotted as the open triangles in Fig. 2 [Note that the corresponding ν_{os}(calc) values are also slightly smaller, as a minor additional consequence of the adjustment in ΔG^*_{os}, Eq. (7)].

The resulting ν_n(ob) - ν_{os}(calc) correlation is similar to that observed using the original ΔG^*_{os} estimates (closed triangles), only with a slightly smaller logarithmic slope (ca. 0.75 versus 0.85). This slope change stems from the tendency of the solvents having smaller r_L^{-1} [and hence ν_{os}(calc)] to also yield smaller ΔG^*_{os} values (Table II),[30] so that

the difference between the two sets of ν_n(ob) estimates tends to diminish with decreasing ν_{os}(calc). Most importantly, however, the analysis indicates that the form of the ν_n(ob) - ν_{os}(calc) correlations are insensitive to the likely uncertainties in the ΔG^*_{os} values employed to estimate ν_n(ob) from k_{ex}.

Activation Parameters

Having deduced the presence of substantial reactivity differences between the various metallocene couples as well as establishing at least a crude dependence on the solvent dynamics, it is of interest to ascertain if these effects are reflected in the preexponential factor derived from activation parameter measurements. Table IV contains a summary of such data for $Cp_2Co^{+/o}$, $Cp_2Fe^{+/o}$, and $Cp'_2Fe^{+/o}$ self exchange, expressed as activation enthalpies, ΔH^*_{ex}, and preexponential factors, A_{ex}, extracted using

$$k_{ex} = A_{ex} \exp (- \Delta H^*_{ex}/RT) \qquad (8)$$

The ΔH^*_{ex} (kcal mol^{-1}) and A_{ex} ($\underline{M}^{-1}$ s^{-1}) values for $Cp_2Co^{+/o}$ self exchange were obtained in the present work (see footnotes to Table IV for details), whereas those for $Cp_2Fe^{+/o}$ and $Cp'_2Fe^{+/o}$ self exchange were extracted from data in ref. 5.[32] The relatively narrow (ca. 30-50 deg) temperature range that was feasible to employ for the present measurements limited the precision of the ΔH^*_{ex} values to about $\pm$ 0.2-0.5 kcal mol^{-1}. Although most values for $Cp_2Co^{+/o}$ given in Table IV refer to solutions containing 0.1 $\underline{M}$ Et_4NBF_4, the variation of ΔH^*_{ex} with ionic strength, μ, for $0 < \mu < 0.14$ (at least in acetonitrile and DMSO) was found to be relatively small (Table

IV). This facilitates comparison with the corresponding activation parameters for $Cp_2Fe^{+/o}$ and $Cp'_2Co^{+/o}$ self exchange, also given in Table IV (taken from ref. 5a) that were obtained for $\mu \sim 0$, especially since these values display a similarly small dependence on ionic strength.[5b]

Table IV also contains the corresponding calculated activation parameters, $\Delta H^*_{ex}(calc)$ and $A_{ex}(calc)$, in each solvent, obtained using the following procedure (outlined in greater detail in ref. 1b). The $\Delta H^*_{ex}(calc)$ values were obtained from

$$\Delta H^*_{ex}(calc) = \Delta G^*_{os} + \Delta G^*_{is} + T\Delta S^* - \Delta H^*_{\tau} \qquad (9)$$

with ΔG^*_{is} taken as 0.5 kcal mol^{-1}, and ΔG^*_{os} obtained from Eq. (4) as before. The intrinsic activation entropy ΔS^* was taken as zero, given that very small values are obtained not only from the dielectric continuum model but also from a phenomenological approach which accounts for specific reactant-solvent interactions.[1b,32] The final term in Eq. (9), ΔH^*_{τ}, accounts for the contribution to the apparent activation enthalpy from the temperature dependence of ν_{os}.[1b] This term is obtained from[1b]

$$\Delta H^*_{\tau} = -R\ (d\ \ln\ \tau_L^{-1}/dT^{-1}) \qquad (10)$$

Unfortunately, temperature-dependent τ_D (and hence τ_L) values are only available for about one half of the solvents considered here, namely acetonitrile, acetone, methanol, DMF,[1b] $(CH_2Cl)_2$,[14] pyridine,[15] and nitromethane.[18] With the exception of methanol, for which ΔH^*_{τ} - 3 kcal mol^{-1}, all these values lie around 1-1.5 kcal mol^{-1} (see Table III here and Table II of ref. 1b for details). Given that methanol exhibits complications from multiple dielectric relaxations[1c] (vide infra), we omit

calculations for this solvent and assume in Table IV that $\Delta H_r^* \sim 1$ kcal mol^{-1} for all solvents where ΔH_r^* is unknown. The corresponding A_{ex}(calc) values in Table IV were then obtained from ΔH_{ex}^*(calc) and k_{ex}(calc) (Table II).

Comparison between the corresponding experimental and calculated activation parameters in Table IV shows that generally $\Delta H_{ex}^* < \Delta H_{ex}^*$(calc) and $A_{ex} < A_{ex}$(calc). This result, noted earlier for $Cp_2Fe^{+/o}$ and $Cp_2'Fe^{+/o}$,[5a] is also obtained for $Cp_2Co^{+/o}$ self exchange. In a given solvent the A_{ex} values are generally larger for the last reaction, indicating that the greater k_{ex} values obtained for $Cp_2Co^{+/o}$ versus $Cp_2Fe^{+/o}$ (Table I) are reflected partly in the preexponential component.

DISCUSSION

Sensitivity of Solvent-Dependent Kinetics to Reactant Structure

A feature of the above results is the differences in the solvent-dependent kinetics observed for the four metallocene self-exchange reactions considered here, as well as in the individual rate constants in a given solvent. In a recent analysis of the latter, we concluded that the larger values of k_{ex} for $Cp_2Co^{+/o}$ versus $Cp_2Fe^{+/o}$, and for $Cp_2'Co^{+/o}$ versus $Cp_2'Fe^{+/o}$ self exchange are due predominantly to greater donor-acceptor orbital overlap for the cobaltocene relative to the ferrocene systems.[6] Thus the $4e_{1g}$ orbital involved in the $Cp_2Co^{+/o}$ reaction is extensively delocalized onto the cyclopentadienyl rings, whereas the $4e_2$ or $8a_{1g}$ orbital employed for the $Cp_2Fe^{+/o}$ electron transfer is almost entirely localized within the iron center. Consequently, the degree of donor-acceptor orbital overlap is expected to be smaller for the latter reaction.

On this basis, then, one might perceive the observed rate differences between $Cp_2Co^{+/o}$ and $Cp_2Fe^{+/o}$ to be due simply to a correspondingly smaller transmission coefficient, κ_{el}, (i.e. lower electron-tunneling probability) for the latter reaction [Eq. (3)]. A somewhat modified picture, however, emerges when the solvent-dependent data in Figs. 1-3 additionally are considered. Although less clearcut than for $Cp_2'Co^{+/o}$ (Fig. 2), the rough correlations seen between ν_n(ob) and ν_{os}(calc) for $Cp_2Co^{+/o}$ and $Cp_2Fe^{+/o}$ self exchange (Figs. 1, 3) indicate that the barrier-crossing frequency for both these reactions is at least partly controlled by the dynamics of solvent reorganization. However, if the observed differences in k_{ex} between the latter two reactions arise directly from differences in κ_{el}, then this necessarily implies that at least the slower $Cp_2Fe^{+/o}$ reaction is distinctly nonadiabatic ($\kappa_{el} \leq 0.1$) in most solvents.

By their very nature, the influence of solvent dynamics (or other nuclear motion) upon the barrier-crossing frequency for such nonadiabatic pathways will be severely muted or eliminated, to an extent which depends upon the magnitude of ν_n. For nonadiabatic pathways having a given donor-acceptor orbital overlap (i.e., for a specific matrix coupling element H_{12}), κ_{el} will decrease as ν_n increases so that eventually κ_{el} should be inversely proportional to ν_n, i.e. k_{ex} is *independent* of ν_n. This circumstance signals complete control of the barrier-crossing frequency by "electronic" rather than nuclear motion.[19a] (See ref. 8 for some illustrative model calculations.) As a consequence, reactions having sufficiently small H_{12} values so to yield substantially nonadiabatic pathways in a given solvent should also yield kinetics that are insensitive to or even entirely independent of the solvent dynamics.

The apparent persistence of solvent dynamical effects for $Cp_2Fe^{+/o}$ self exchange can nonetheless be rationalized by considering the likely variations in κ_{el} for different spatial configurations of the precursor complex. Given that the metal-centered $4e_g$ (or $8a_{1g}$) orbital involved in $Cp_2Fe^{+/o}$ self exchange features lobes parallel to the Cp rings, significant donor-acceptor overlap may well be possible for precursor complex geometries featuring a "side-by-side" reactant approach (i.e. with the Cp rings for both reactants oriented in the same plane). If H_{12} is sufficiently large so to yield adiabatic reaction channels within such precursor geometries, yet sufficiently small for other configurations (such as those involving a common five-fold axis) so that then $\kappa_{el} \ll 1$, the situation can be described simply by the addition of a multiplicative fractional "steric factor", ρ, into the K_p expression [Eq. (5)], with κ_{el} in Eq. (3) maintained as unity. While the assumption of reactant sphericity in Eq. (5) is an obvious oversimplification, considerations of the fractional reactant "surface area" corresponding to such "side-by-side" precursor geometries yield ρ values of 0.1 or less. Such steric effects therefore can account readily for the tenfold smaller reactivities of $Cp_2Fe^{+/o}$ versus $Cp_2Co^{+/o}$ observed in a number of solvents (Table I). Such factors may well also be responsible for the similarly disparate exchange rates of $Cp'_2Co^{+/o}$ versus $Cp'_2Fe^{+/o}$ (Table I).

The extremely facile self-exchange kinetics for $Cp'_2Co^{+/o}$, together with the good correlation observed between $\nu_n(ob)$ and $\nu_{os}(calc)$ (Fig. 2), are suggestive that this system involves sufficiently strong donor-acceptor electronic coupling so to yield adiabatic reaction channels for most precursor complex geometries featuring suitably close internuclear

distances. In other words, it is likely that most internuclear configurations featuring reasonable proximity of the reactants will provide viable electron transfer pathways. Conversely, the distinctly poorer correlation (and milder dependence) of ν_n(ob) with ν_{os}(calc) observed in Fig. 1 for $Cp_2Co^{+/o}$ self exchange is suggestive of the presence of solvent-dependent steric effects. In this regard, it might be viewed as surprising that the ν_n(ob) - ν_{os}(calc) correlation observed for $Cp_2Fe^{+/o}$ (Fig. 3, circles) displays less scatter than that for the more facile $Cp_2Co^{+/o}$ reaction (Fig. 1, circles). This is, however, probably due in part to the differing selection of solvents involved in these two plots.

Broadly speaking, the experimental activation parameters for $Cp_2Co^{+/o}$ and $Cp_2Fe^{+/o}$ (Table IV) are consistent with these interpretations. The larger preexponential factors observed for $Cp_2Co^{+/o}$ versus $Cp_2Fe^{+/o}$ in a given solvent are in reasonable accordance with the larger K_p (and/or κ_{el}) values anticipated for the former reaction. However, comparison with the corresponding calculated activation parameters, ΔH^*_{ex}(calc) and A_{ex}(calc), in Table IV indicates that other obfuscating factors are present. Not only are the experimental A_{ex} factors typically substantially smaller than the corresponding A_{ex}(calc) values, but the solvent dependence of A_{ex} does not match that of A_{ex}(calc). For $Cp_2Co^{+/o}$ self exchange, the A_{ex} values do not vary greatly between most solvents, whereas the solvent dependence of A_{ex}(calc) is substantial and reflects chiefly the corresponding variations in ν_{os}(calc), as a consequence of Eq. (7). Correspondingly, the differences between ΔH^*_{ex} and ΔH^*_{ex}(calc) are also large and systematic, with the former being ca. 2-3 kcal mol^{-1} smaller than the latter (Table IV).

This observation that $\Delta H^*_{ex} < \Delta H^*_{ex}$(calc) and $A_{ex} < A_{ex}$(calc) (or,

equivalently, the occurrence of unexpectedly negative activation entropies, ΔS^{*}_{ex}) has been noted for a variety of other homogeneous-phase redox processes, most commonly involving cationic transition-metal complexes in aqueous solution.[33] This behavior is thought to reflect the enthalpic and entropic components of the precursor complex formation constant, K_p, rather than the energetics of the electron-transfer step itself. Given that formation of the precursor state from the isolated reactants almost inevitably necessitates significant mutual modifications in their solvation (vide supra) it would not be surprising if these changes involve sizable (and compensating) enthalpic and entropic components. It is, nonetheless, noteworthy that such effects persist even for the present systems, which involve monocation-neutral reactant pairs featuring relatively weak and nonspecific solute-solvent interactions.

Functional Dependence of Kinetics upon Solvent Dynamics

A major hoped-for objective in detailed experimental studies such as are described here is to utilize solvent-dependent kinetic data to test the extent to which the solvent continuum model provides a satisfactory description of the barrier-crossing dynamics. In addition, it is of interest to ascertain to what extent the solvent influence upon the barrier-crossing frequency, $\nu_n\kappa_{el}$, is muted by the presence of reactant vibrational (i.e. inner-shell contributions) to ν_n, as well as by possible nonadiabaticity effects (i.e. $\kappa_{el} \ll 1$) as noted above. The relative importance of inner- and outer-shell motion to ν_n is a question of some importance since for most electron-transfer reactions both these types of modes contribute significantly to the free-energy barrier.

Marcus and coworkers have recently presented a theoretical treatment which incorporates the influence of reactant vibrations as well as overdamped solvent polarization in descriptions of the reaction dynamics.[2f,g] Generally speaking, the effect of the typically faster vibrational mode will be to increase the adiabatic barrier-crossing frequency, ν_n, to an extent which depends upon the relative inner- and outer-shell contributions to the barrier, $\Delta G^*_{is}/\Delta G^*_{os}$, together with the corresponding relative frequencies, ν_{is}/ν_{os}.[34] As a consequence, in the presence of a significant vibrational reaction coordinate, i.e., for $\Delta G^*_{is} > 0$, the dependence of ν_n upon ν_{os} for a given reaction in a series of solvents (or, approximately, for ν_n versus τ_L^{-1}) will be diminished, and therefore take the form of an approximate fractional power law, so that roughly $\nu_n \propto \nu_{os}^{\alpha}$ with $0 < \alpha < 1$.[2g]

As noted above, the present systems feature small yet significant inner-shell barriers ($\Delta G^*_{is} \approx 0.5$ kcal mol^{-1}) so that in all solvents examined here, $\Delta G^*_{is}/\Delta G^*_{os} \approx 0.1$. Given that $Cp'_2Co^{+/o}$ self exchange exhibits a good correlation between ν_n(ob) and ν_{os}(calc) (Fig. 2), it is of interest to ascertain if such a power-law dependence is predicted for this system. From Fig. 7 of ref. 2g, the vertical displacement between the plots for nonzero "λ_i/λ_o" values (equal to $\Delta G^*_{is}/\Delta G^*_{os}$ in the present notation) and that for $\lambda_i/\lambda_o = 0$ denotes the increase in log ν_n caused by the presence of the vibrational coordinate for a given x-axis value of log τ_L. Applying these numerical results[36] within the range of solvents considered for $Cp'_2Co^{+/o}$ in Fig. 2 [i.e. for τ_L values from 0.2 ps (acetonitrile) to 8.9 ps (HMPA)], and assuming that $\Delta G^*/RT = 9$, $\nu_{is} = 9 \times 10^{12}$ s^{-1}[1b,6] and $\Delta G^*_{is}/\Delta G^*_{os} = 0.1$, yields an approximately linear plot of log ν_n versus log

ν_n with a slope of about 0.67, (i.e. the predicted power-law coefficient, $\alpha = 0.67$).

The best-fit slopes of the two log ν_n(ob) - log ν_{os}(calc) plots shown in Fig. 2 are about 0.85 and 0.7 for the filled and open points, respectively. Given the above arguments supporting the approximate validity of the latter plot, the form of Fig. 2 may be taken as evidence supporting at least the qualitative validity of the fractional "power-law" dependence predicted in ref. 2g. This interpretation should be tempered with caution considering the inevitable assumptions required for the experimental data analysis. Nevertheless, the significant predicted influence upon the ν_n values by the reactant vibrational coordinate, even for systems displaying relatively small inner-shell barriers, is interesting and worthy of further experimental examination.

Irrespective of the detailed functional form of the ν_n(obs)-ν_{os}(calc) relationship, the good correlation between the quantities observed in Fig. 2 provides direct evidence that at least the relative values of ν_{os} for the majority of solvents are close to (within 1.5-2 fold of) those estimated from the simple overdamped continuum model embodied in Eq. (7). Some interesting deviations nevertheless occur. Most obviously, the ν_n(ob) value for $Cp_2'Co^{+/o}$ in propylene carbonate is about fourfold larger than anticipated on this basis (Fig. 2). A qualitatively similar deviation is also seen for $Cp_2Co^{+/o}$ in this solvent (Fig. 1); in addition the ν_n(ob) values obtained for this reaction in NMF and especially methanol (Fig. 1) are substantially larger than expected. A similar observation applies to both $Cp_2Co^{+/o}$ electrochemical exchange and $Cp_2Fe^{+/o}$ self exchange in methanol (Fig. 1, 3).

These unexpectedly large $\nu_n(ob)$ values could possibly arise from the estimates of ΔG^*_{os} or K_p employed to extract them from the experimental k_{ex} values being too small or large, respectively, relative to the corresponding estimates in the remaining solvents. At least for methanol and propylene carbonate, however, the E_{op} data shows no evidence of ΔG^*_{os} values that are abnormally small relative to the dielectric continuum expectations.[27,28a,37] The occurrence of anomalous K_p values is also considered unlikely, especially for methanol, since similarly large deviations are found for two different probe reactions and in electrochemical as well as homogeneous-phase environments. Most likely, then, the surprisingly large $\nu_n(ob)$ values in these media reflect effective solvent relaxation times, τ_{eff}, that are correspondingly smaller than the values, τ_L, extracted from the dielectric continuum treatment [Eq. (7)].

The most likely origin of this discrepancy for alcohol solvents appears to lie in dominant contributions to τ_{eff} from -OH group rotations.[1c] Such motions are associated with substantially shorter relaxation times (ca. 1 ps) than for the predominant relaxation mode. Although the former is a relatively minor component of the overall dielectric polarization, such motions can nonetheless exert a disproportionately large influence upon τ_{eff} for barrier crossing, especially for the cusp-like ("sharp") barriers expected for weakly adiabatic outer-sphere processes.[2e]

The influence of such high-frequency components of the dielectric polarization may also be responsible for the apparent finding that $\tau_{eff} \ll \tau_L$ for the other solvents noted above. It is tempting to ascribe the occurrence of this phenomenon to "hydrogen-bonding effects" (cf. ref. 4d),

especially since NMF as well as methanol engages in extensive H-bonding. However, this leaves unanswered the precise nature of the high-frequency motion responsible. For propylene carbonate, an additional relaxation having a significantly higher frequency than the major mode has been identified in the dielectric loss spectra;[38] this may account at least in part for the finding that $\tau_{eff} < \tau_L$ in this solvent. Nevertheless, a central problem with dielectric loss measurements for this purpose is that the detection of such high-frequency relaxations can be difficult and ambiguous.[39]

The recent emergence of picosecond time-resolved measurements of fluorescence Stokes shifts involving polar excited states of suitable dye solutes[40] are of great interest in this regard, since they can provide direct real-time information on the solvation dynamics. The data reported so far indicate that the measured solvation times, τ_s, in simple aprotic solvents tend to be somewhat longer than τ_L, although the relative τ_s values are roughly proportional to τ_L.[40] Considering that only relative, rather than absolute, τ_{eff} values are accessible from the k_{ex} measurements due to the need to correct for the electron-transfer barrier, these findings are broadly consistent with the results presented here. A more detailed comparison of polar solvent dynamics as inferred from electron-transfer kinetics and time-resolved fluorescence measurements will be given elsewhere.[41]

Concluding Remarks

The present results add significantly to the extant experimental evidence attesting to the appropriateness of theoretical rate expressions

that include a solvent-dependent barrier-crossing frequency.[1,4] While the observed behavior is in some respects consistent with the predictions of the simple "overdamped" solvent continuum model, several unexpected features have emerged which are worthy of attention. The dominant influence of solvent dynamics upon the barrier-crossing frequency appears to persist even for reactions, such as $Cp_2Fe^{+/o}$ self exchange, where the reaction rates are retarded substantially by weak donor-acceptor electronic coupling. A related point concerns the retention of overdamped solvent dynamical behavior even in solvents, such as acetonitrile, that feature sufficiently rapid dielectric relaxation so that nonadiabaticity and/or solvent inertial effects might be expected instead to control the barrier-crossing frequency.[42]

In addition, the effective barrier-crossing frequencies for the present reactions in a significant number of solvents are substantially (up to ca. 100 fold) faster than expected from solvent relaxation data, with effective ν_n values that may well approach 10^{13} s^{-1}. Generally speaking, contributions from reactant vibrations as well as solvent motions should be considered even though the reactions studied here were chosen to minimize the former. While this inner-shell contribution can be significant, at least when $\nu_{is} >> \nu_{os}$, such modes do not appear to provide a dominant contribution to barrier-crossing frequency for the present systems. Given the likely importance of solvent high-frequency modes to outer-sphere reaction rates, identifying and understanding the molecular dynamics involved would appear to be a problem of some significance.

ACKNOWLEDGMENTS

Helpful insight regarding reactant vibrational effects was provided by Dr. Walter Nadler. This work is supported by the Office of Naval Research. The nmr instruments used in this work are supported by National Institute of Health Grant RR 01077 at Purdue University. G.E.M. gratefully acknowledges partial financial support from a Department of Navy Graduate Research Fellowship.

Supplementary Material Available:

Tables of proton nmr and related parameters for $Cp_2Co^{+/o}$, $Cp_2'Co^{+/o}$, and $Cp_2'Fe^{+/o}$ self exchange in the various solvent systems employed in this work, at varying temperatures (six pages). Ordering information is given on any current masthead page.

REFERENCES AND NOTES

1. (a) Weaver, M. J.; and Gennett, T., Chem. Phys. Lett. 1985, 113, 213; (b) Gennett, T.; Milner, D. F.; and Weaver, M. J., J. Phys. Chem. 1985, 89, 2787; (c) McManis, G. E.; Golovin, M. N.; and Weaver, M. J., J. Phys. Chem. 1986, 90, 6563.

2. (a) Calef, D. F.; and Wolynes, P. G., J. Phys. Chem. 1983, 87, 3387; (b) Zusman, L. D., Chem. Phys. 1980, 49, 295; (c) Alexandrov, I. V., Chem. Phys. 1980, 51, 499; (d) Van der Zwan, G.; and Hynes, J. T., J. Phys. Chem. 1985, 89, 4181; (e) Hynes, J. T., J. Phys. Chem. 1986, 90, 3701; (f) Sumi, H.; and Marcus, R. A., J. Chem. Phys. 1986, 84, 4894; (g) Nadler, W.; and Marcus, R. A., J. Chem. Phys. 1987, 86, 3906.

3. Gennett, T.; and Weaver, M. J., J. Electroanal. Chem. 1985, 186, 179.

4. For example, (a) Harrer, W.; Grampp, G.; and Jaenicke, W., Chem. Phys. Lett. 1984, 112, 263; (b) Kapturkiewicz, A.; and Opallo, M., J. Electroanal. Chem. 1985, 185, 15; (c) Opallo, M.; and Kapturkiewicz, A., Electrochim. Acta 1985, 30, 1301; (d) Opallo, M., J. Chem. Soc. Far. Trans I 1986, 82, 339.

5. (a) Yang, E. S.; Chan, M.-S.; and Wahl, A. C., J. Phys. Chem. 1980, 84, 3094; (b) Yang, E. S.; Chan, M.-S.; and Wahl, A. C., J. Phys. Chem. 1975, 79, 2049.

6. Nielson, R. M.; McManis, G. E.; Golovin, M. N.; and Weaver, M. J., J. Am. Chem. Soc., in press.

7. McManis, G. E.; Nielson, R. M.; and Weaver, M. J., Inorg. Chem., submitted.

8. McManis, G. E.; Mishra, A. K.; and Weaver, M. J., J. Chem. Phys. 1987, 86, 5550.

9. Kölle, U.; and Khouzami, F., Chem. Ber. 1981, 114, 2929.

10. Perrin, D. D.; Armarego, W. L. F.; and Perrin, D. R., "Purification of Laboratory Chemicals", 2nd Ed., Pergamon, New York, 1980.

11. Van Geet, A. L., Anal. Chem. 1970, 42, 679; 1968, 40, 2227.

12. Riddick, J. A.; and Bunger, W. B., "Organic Solvents", Wiley-Interscience, New York, 1970.

13. Calderwood, J. H.; Smyth, C. P., J. Am. Chem. Soc. 1956, 78, 1295.

14. Hennelly, E. J.; Heston, W. M.; Smyth, C. P., J. Am. Chem. Soc. 1948, 70, 4102.

15. Holland, R. S.; and Smyth, C. P., J. Phys. Chem. 1955, 59, 1088.

16. Poley, J. P., App. Sci. Res. B 1955, 4, 337.

17. Behret, H.; Schmittals, F.; and Barthel, J., Z. Physik. Chem. 1975, 96, 73.

18. Chandra, S.; and Nath, D., J. Chem. Phys. 1969, 51, 5299.

19. (a) For a review, see Sutin, N., Prog. Inorg. Chem. 1983, 30, 441. (b) Hupp, J. T.; and Weaver, M. J., J. Electroanal. Chem. 1983, 152, 1.

20. Marcus, R. A., J. Chem. Phys. 1965, 43, 679.

21. The value $\delta r = 0.6$ Å is somewhat arbitrary. For spherical reactants, δr can be related to the dependence of κ_{el} upon the internuclear distance, which takes the form[22] $\kappa_{el}(r) = \kappa_{el}^{\circ} \exp[-\alpha(r - \sigma)]$ where σ is the separation distance corresponding to the closest approach, having the transmission coefficient κ_{el}°. Taking $\alpha \sim 1.5$ Å (a reasonable estimate[22]), one can deduce that κ_{el} falls to κ_{el}°/e for $(r - \sigma) = \delta r = \alpha^{-1}$, i.e. ca. 0.6 Å.

22. For example, (a) Newton, M., ACS Symp. Ser 1982, 198, 255; (b) Newton, M., J. Phys. Chem. 1986, 90, 3734.

23. For example, (a) Frolich, H., "Theory of Dielectrics", Oxford University Press, London, 1949; (b) Hubbard, J. B., J. Chem. Phys. 1978, 68, 1649.

24. Our approximate calculations of the influence of solvent inertial effects in ref. 1b suggest that significant deviations from complete overdamped behavior occur for several solvents considered here. These calculations employed a relation due to Calef and Wolynes[2a] which presumes the solvent medium to be nonpolarizable (i.e. $\epsilon_{\infty} = \epsilon_{op} = 1$). However, significantly different relationships result when solvent

polarity and polarizability are taken into account. This matter will be discussed in detail elsewhere.

25. The ΔG^*_{is} values for the electrochemical exchange reaction will be one half that for the corresponding homogeneous self-exchange process since only one redox center is required to be activated for the former, versus two for the latter. The equality of the ΔG^*_{os} values for the corresponding electrochemical and homogeneous exchange processes follows from the assumption made here and in ref. 1b that the reacting pair are in contact for the latter, so that a = 0.5R in Eq. (4), whereas the reactant-electrode image interaction can, to a first approximation, be neglected for the former process. These combined factors lead to a cancellation of the otherwise-expected twofold difference in ΔG^*_{os} values between the electrochemical and homogeneous-phase reactions.

26. For a review, see Creutz, C., Prog. Inorg. Chem. 1983, 30, 1.

27. For example, Hupp, J. T.; and Meyer, T. J., Inorg. Chem. 1987, 26, 2332.

28. (a) Powers, M. J.; and Meyer, T. J., J. Am. Chem. Soc. 1978, 100, 4393; (b) McManis, G. E.; and Weaver, M. J., in preparation.

29. Wolynes, P. G., J. Chem. Phys. 1987, 86, 5133.

30. This crude correlation between r_L^{-1} and ΔG^*_{os} can be traced to the tendency of the smaller and hence dynamically faster solvents (i.e., larger r_L^{-1}) to be less polarizable, giving rise to smaller ϵ_{op} and therefore larger ΔG^*_{os} values.

31. The values of ΔH^*_{ex} for $Cp_2Fe^{+/o}$ and $Cp'_2Fe^{+/o}$, extracted from ref. 5, are those given as "E_a" in ref. 5a. The other "ΔH^*" values reported in ref. 5a are smaller than E_a by a factor of 0.5 RT, supposedly to account for the temperature dependence of the "collisional frequency". These latter values are not appropriate when using the encounter preequilibrium treatment embodied in Eq. (3).[19b]

32. Hupp, J. T.; and Weaver, M. J., J. Phys. Chem. 1984, 88, 1860.

33. For example, see (a) Taube, H., "Electron Transfer Reactions of

Complex Ions in Solution", Academic Press, 1970, Chapter III; (b) Weaver, M. J.; and Yee, E. L., Inorg. Chem. 1980, 19, 1936; (c) Hupp, J. T.; and Weaver, M. J., J. Phys. Chem. 1985, 89, 2795.

34. A slightly different interpretation of the anticipated effect of the vibrational coordinate upon ν_n was given in ref. 1b, based on the results of an earlier simplified theoretical treatment.[35] The more exhaustive treatment given in refs. 2f and g has greater relevance to the experimental situation at hand, although is still incomplete. (For example, it employs cusp-shaped barriers, assumes complete adiabaticity, and does not consider reverse barrier crossings.)

35. Ovchinnokova, M. Ya., Russ. Theoret. Exp. Chem. 1981, 17, 507.

36. The procedure involves noting that the "normalization" rate constant, k_e, in ref. 1g is related to the vibrational frequency, ν_{is}, by Eq. (2.9) of ref. 1g: $k_e = \nu_{is} (1 + \Delta G^*_{os}/\Delta G^*_{is})^{-\frac{1}{2}} \exp(\Delta G^*/RT)$ [using present notation]. This enables the x-axis of the plots in Fig. 7 in ref. 2g to be transformed to log τ_L, and hence to log ν_{os}, for given values of ν_{is}, ΔG^*_{is}, and ΔG^*_{os}.

37. Creutz, C., Inorg. Chem. 1978, 17, 3723.

38. Cavell, E. A. S., J. Chem. Soc. Far. Trans. II, 1974, 70, 78.

39. Hill, N. E.; Vaughan, W. E.; Price, A. H.; Davies, M., "Dielectric Properties and Molecular Behavior", Van Nostrand Reinhold, London, 1969.

40. (a) Castner, E. W., Jr.; Maroncelli, M.; and Fleming, G. R., J. Chem. Phys. 1987, 86, 1090; (b) Maroncelli, M.; and Fleming, G. R., J. Chem. Phys. 1987, 86, 6221; Kahlow, M. A.; Kang, T. J.; and Barbara, P. F., J. Chem. Phys., in press.

41. McManis, G. E.; and Weaver, M. J., Chem. Phys. Lett., submitted.

42. A consideration of nuclear-tunneling factors may well account for the lack of nonadiabaticity effects under these conditions.[43]

43. Gochev, A., work in progress.

TABLE I. Summary of Rate Constants, k_{ex}, for Metallocene Self-Exchange Reactions at 25°C.

Solvent[a]	10^{-7} k_{ex} M^{-1} s^{-1}[b]				k_{ex}/k_{ex}^{ACN}[d]				$(k_{ex}/k_{ex}^{ACN})_{calc}$[e]
	$Cp_2Co^{+/o}$	$Cp_2'Co^{+/o}$	$Cp_2Fe^{+/o}$	$Cp_2'Fe^{+/o}$	$Cp_2Co^{+/o}$	$Cp_2'Co^{+/o}$	$Cp_2Fe^{+/o}$	$Cp_2'Fe^{+/o}$	
1. Acetonitrile	3.8	43	0.53	3.8	--	--	--	--	
2. Acetone	1.9	22.5	0.46	2.4	0.50	0.5	0.87	0.63	1.05
3. CH_2Cl_2	8.9		0.43	4.4	2.3		0.81	1.15	5.1
4. $(CH_2Cl)_2$	6.3		0.43		1.6		0.81		1.4
5. Pyridine	4.5			3.9[c]	1.2			1.0	2.3
6. DMF	2.6	20			0.7	0.45			0.39
7. DMSO	2.4	18.5	0.16		0.65	0.43	0.30		0.34
8. PC	2.9	28			0.75	0.65			0.14
9. Benzonitrile	6.1	24.5		5.0[c]	1.6	0.57		1.32	0.35
10. Nitrobenzene			0.23				0.43		0.38
11. TMU	1.25				0.3				0.16
12. HMPA	0.54	3.5			0.14	0.08			0.1
13. Methanol	7.2		0.6		1.9		1.13		(0.02)
14. Nitromethane			0.58				1.1		1.4
15. NMF	6.7				1.8				0.1

Footnotes to Table I

[a] DMF = N,N-dimethylformamide; DMSO = dimethylsulfoxide; PC = propylene carbonate; TMU = tetramethylurea; HMPA = hexamethylphosphoramide; NMF = N-methylformamide.

[b] Measured rate constant for self exchange of cobalt and iron metallocenes in indicated solvent as obtained by proton nmr line broadening; Cp = cyclopentadienyl; Cp' = pentamethyl-cyclopentadienyl. Values listed for $Cp_2Co^{+/o}$ and $Cp'_2Co^{+/o}$ were obtained in this work, solutions contained 0.04 M Cp_2Co^+ or Cp'_2Co^+ and 0.1 M Et_4NBF_4. Reproducibility of values quoted generally within ca. 5-10%. Values for $Cp_2Fe^{+/o}$ and $Cp'_2Fe^{+/o}$ were taken from ref. 5a, unless noted otherwise; solutions contained no added supporting electrolyte. (See text and Supplementary Material for further details.)

[c] Value obtained in this work.

[d] Ratio of self-exchange rate constant for given metallocene redox couple measured in indicated solvent to corresponding value obtained in acetonitrile; values taken from adjacent left-hand columns.

[e] Calculated ratio of self-exchange rate constant to that in acetonitrile, obtained from values of k_{ex} listed in Table II. Values given in parentheses for methanol and propylene carbonate are expected to be in error due to presence of multiple dielectric relaxations. (See footnotes to Table II and text for further details.)

TABLE II Calculated Rate Parameters for $Cp_2M^{+/o}$ Self Exchange at 25°C

No.	Solvent[a]	τ_L[b] 10^{-12} s	ν_{os}(calc)[c] 10^{12} s^{-1}	ΔG^*_{os}[d] kcal mol^{-1}	k_{ex}(calc)[e] $\underline{M}^{-1}$ s^{-1}	k^f_{ex}(calc)[f] $\underline{M}^{-1}$ s^{-1}
1	Acetonitrile	~0.2	5	5.75	3.5×10^7	7×10^7
2	Acetone	0.3	3.0	5.4	3.7×10^7	1.2×10^8
3	CH_2Cl_2	~0.4	1.9	4.2	1.8×10^8	9.3×10^8
4	$(CH_2Cl)_2$	1.6	0.45	4.15	4.8×10^7	1.0×10^9
5	Pyridine	1.2	0.6	4.0	7.8×10^7	1.3×10^9
6	DMF	1.3	0.6	5.05	1.3×10^7	2.2×10^8
7	DMSO	2.4	0.34	4.8	1.2×10^7	3.4×10^8
8	PC	2.7	0.31	5.25	4.8×10^6	1.6×10^8
9	Benzonitrile	5.8	0.13	4.2	1.2×10^7	9.3×10^8
10	Nitrobenzene	5.2	0.14	4.2	1.3×10^7	9.3×10^8
11	TMU	~6	0.15	4.75	5.6×10^6	3.7×10^8
12	HMPA	8.9	0.09	4.75	3.3×10^6	3.7×10^8
13	Methanol	(8.2)	(0.11)	5.85	(6.5×10^5)	5.8×10^7
14	Nitromethane	0.2	4	5.4	4.8×10^7	1.2×10^8
15	NMF	3.7	0.23	5.3	3.4×10^6	1.5×10^8

Footnotes to Table II

[a] DMF = N,N-dimethylformamide; DMSO = dimethylsulfoxide; PC = propylene carbonate; TMU = tetramethylurea; HMPA = hexamethylphosphoramide; NMF = N-methylformamide.

[b] Longitudinal solvent relaxation time, calculated from corresponding values of τ_D, ϵ_s, and ϵ_∞ by using Eq. (7a). See Table III and ref. 1c (Table II) for further details and literature sources.

[c] Effective nuclear barrier-crossing frequency due to overdamped solvent motion according to dielectric continuum model, obtained from corresponding listed τ_L and ΔG^*_{os} values by using Eq. (7). Value for methanol anticipated to be in error due to presence of multiple dielectric relaxation (see text).

[d] Activation energy for $Cp_2M^{+/o}$ self exchange due to solvent reorganization according to dielectric continuum model, obtained from Eq. (4) assuming that a = 3.8 Å, 2a = R, with values of ϵ_{op} and ϵ_s for the various solvents taken from Table III and ref. 1c (Table II).

[e] Calculated rate constant for $Cp_2M^{+/o}$ self exchange, obtained from Eq. (3) with $K_p = 0.26\ M^{-1}$, $\kappa_{el} = 1$, $\Delta G^*_{is} = 0.5$ kcal mol^{-1}, assuming that $\nu_n = \nu_{os}$ and using the values of ν_{os} and ΔG^*_{os} listed for each solvent in adjacent columns (see text for details).

[f] Calculated rate constant for $Cp_2M^{+/o}$ self exchange, obtained as summarized in footnote e, but assuming that $\nu_n = 1 \times 10^{13}\ s^{-1}$ in each solvent (i.e. using a fixed frequency factor).

TABLE III Dielectric and Related Properties for Additional Solvents Examined Here (see also Table I of ref. 1c)[a]

Solvent[b]	ϵ_{op}[c]	ϵ_s[c]	ϵ_∞[e]	η[f] 10^{-3} Poise	τ_D[g] 10^{-12} s	τ_L[h] 10^{-12} s	ΔH_τ^{*}[i] kcal mol^{-1}
Acetone	1.84	21[j]	−2[j]	3.0	3.3[j]	0.3	1.0[j]
$(CH_2Cl)_2$	2.08	10.2[k]	−2.4[k]	7.8	6.9[k]	1.6	1.5[k]
Pyridine	2.27	13.3[l]	−2.3[l]	8.85	6.9[l]	1.2	1.0[l]
Nitrobenzene	2.40	35.7[m,n]	4.1[m,n]	18.1	45.6[m,n]	5.2	
HMPA	2.12	29.6[o]	3.3[o]	34.7[m]	80[o]	8.9	
Nitromethane	1.90	36[p]	−2[p]	6.1	3.9[p]	0.2	1.0[p]

[a] All data refer to 25°C unless noted otherwise.

[b] $(CH_2Cl)_2$ = 1,2-dichloroethane; HMPA = hexamethylphosphoramide.

[c] Optical dielectric constant, from refractive index data given in ref. 12.

[d] Static dielectric constant, from sources indicated.

[e] "Infinite frequency" dielectric constant, from sources indicated.

[f] Viscosity, from ref. 12.

[g] Debye relaxation time, from sources indicated.

[h] Longitudinal solvent relaxation time, determined from corresponding values of τ_D, ϵ_s, and ϵ_∞ by using Eq. (7a).

[i] Activation enthalpy associated with longitudinal solvent relaxation; determined from temperature-dependent τ_D data, from sources indicated, by using Eq. (10). (Values given to nearest 0.5 kcal mol^{-1}.)

[j] Ref. 13; [k] Ref. 14; [l] Ref. 15; [m] Determined at 20°C; [n] Ref. 16; [o] Ref. 17; [p] Ref. 18.

TABLE IV. Activation Enthalpies, ΔH^*_{ex} (kcal mol^{-1}) and Preexponential Factors, A_{ex} ($\underline{M}^{-1}$ s^{-1}) for Metallocene Self Exchange, and Comparison with Calculated Parameters.

Solvent	$Cp_2Co^{+/o}$		$Cp_2Fe^{+/o}$		$Cp'_2Fe^{+/o}$		ΔH^*_{ex}(calc)[f]	A_{ex}(calc)[g]
	ΔH^*_{ex} [a,c]	A_{ex} [b,c]	ΔH^*_{ex} [a,d]	A_{ex} [b,d]	ΔH^*_{ex} [a,d]	A_{ex} [b,d]		
1. Acetonitrile	4.3	5.0×10^{10}	5.0	2.5×10^{10}	4.0	3.3×10^{10}	7.5	1×10^{13}
	4.6[e]	1.0×10^{11}[e]						
2. Acetone	4.4	3.0×10^{10}	4.8	1.5×10^{10}	3.6	1.0×10^{10}	7.0	5×10^{12}
3. CH_2Cl_2	3.4	2.5×10^{10}	2.0	1.3×10^{8}	3.5	1.5×10^{10}	~6	~1×10^{13}
5. Pyridine	3.9	3.5×10^{10}					5.5	8×10^{11}
7. DMSO	4.8	7.5×10^{10}					6.5	7×10^{11}
	4.7[e]	5.5×10^{10}[e]						
9. Benzonitrile	4.7	2×10^{11}					6.0	3×10^{11}
10. Nitrobenzene			2.3	1.0×10^{8}			6.0	3×10^{11}
12. HMPA	5.6	7×10^{10}					~7	~5×10^{11}
13. Methanol	4.3	1.0×10^{10}	3.0	1.0×10^{9}				
14. Nitromethane			4.0	5×10^{9}			7.0	6×10^{12}

Footnotes to Table IV

[a] Activation enthalpy (kcal mol^{-1}) for self exchange of stated metallocene redox couple in various solvents, determined from temperature dependence of k_{ex} using Eq. (8). Reproducibility for $Cp_2Co^{+/o}$ generally within ± 0.5 kcal mol^{-1}.

[b] Preexponential factor (M^{-1} s^{-1}), determined from temperature dependence of k_{ex} using Eq. (8).

[c] Values obtained in this work, for solutions containing ca. 30 mM $Cp_2Co^{+/o}$ and 0.1 M Et_4NBF_4 unless indicated otherwise.

[d] Values extracted from ref. 5a; obtained in absence of inert electrolyte.

[e] Values obtained for solutions containing ca. 15 mM Cp_2Co^{+} and in absence of inert electrolyte.

[f] Calculated activation enthalpy (kcal mol^{-1}), obtained by using Eq. (9) with ΔG^*_{os} from Eq. (4), ΔG^*_{is} taken as 0.5 kcal mol^{-1}, $\Delta S^* = 0$, and ΔH^*_τ either from Eq. (10) or estimated as noted in the text.

[g] Calculated preexponential factor (M^{-1} s^{-1}), obtained from values of ΔH^*_{ex}(calc) listed alongside together with k_{ex}(calc) (Table II).

Figure Captions

Fig. 1. Logarithmic plot of "observed" nuclear frequency factors, $\nu_n(ob)$, for a series of solvents extracted from k_{ex} values for $Cp_2Co^{+/o}$ self exchange (filled circles), against corresponding calculated frequency factors, $\nu_{os}(calc)$, obtained from overdamped solvent relaxation model [Eq. (7)]. Crosses are corresponding points for $Cp_2Co^{+/o}$ electrochemical exchange at mercury-solvent interface. See text for calculational details. Straight line corresponds to $\nu_n(ob) = \nu_{os}(calc)$. Key to solvents (also as given in Table I): 1, acetonitrile; 2, acetone; 3, dichloromethane; 4, 1,2-dichloroethane; 5, pyridine; 6, N,N-dimethylformamide; 7, dimethylsulfoxide; 8, propylene carbonate; 9, benzonitrile; 10, nitrobenzene; 11, tetramethylurea; 12, hexamethylphosphoramide; 13, methanol; 14, nitromethane; 15, N-methylformamide.

Fig. 2. Logarithmic plots of "observed" nuclear frequency factors, $\nu_n(ob)$, extracted from k_{ex} values for $Cp_2'Co^{+/o}$ self exchange for a series of solvents, against corresponding calculated frequency factors, $\nu_{os}(calc)$, obtained from overdamped solvent relaxation model [Eq. (7)]. Filled triangles refer to $\nu_n(ob)$ values obtained by employing outer-shell barrier ΔG^*_{os} estimated from Eq. (4); open triangles obtained by assuming that the ΔG^*_{os} values are 0.74 times these estimates (see text for details). For key to solvents, see caption to Fig. 1 or Table I.

Fig. 3. Logarithmic plots of "observed" nuclear frequency factors, $\nu_n(ob)$, extracted from k_{ex} values for $Cp_2Fe^{+/o}$ (circles) and $Cp_2'Fe^{+/o}$ self exchange (triangles) for a series of solvents, against corresponding calculated frequency factors, $\nu_{os}(calc)$, obtained from overdamped solvent relaxation model [Eq. (7)]. (See text for details). For key to solvents, see caption to Fig. 1 or Table I.

Fig. 4. Comparison of logarithmic plots of $\nu_n(ob)$ versus $\nu_{os}(calc)$ for $Cp_2Fe^{+/o}$ self exchange (see Fig. 3), with $\nu_n(ob)$ estimated from k_{ex} values using outer-shell barrier ΔG^*_{os} from dielectric continuum model [Eq. (4)] (filled squares) and from observed solvent-dependent intervalence charge-transfer energies, E_{op}, for biferrocenylacetylene cations (open squares). Data for latter taken from ref. 28a, except for 1,2-dichloroethane, for which $E_{op} = 5.75 \times 10^3$ cm^{-1}.[28b] For key to solvents, see caption to Fig. 1 or Table I.

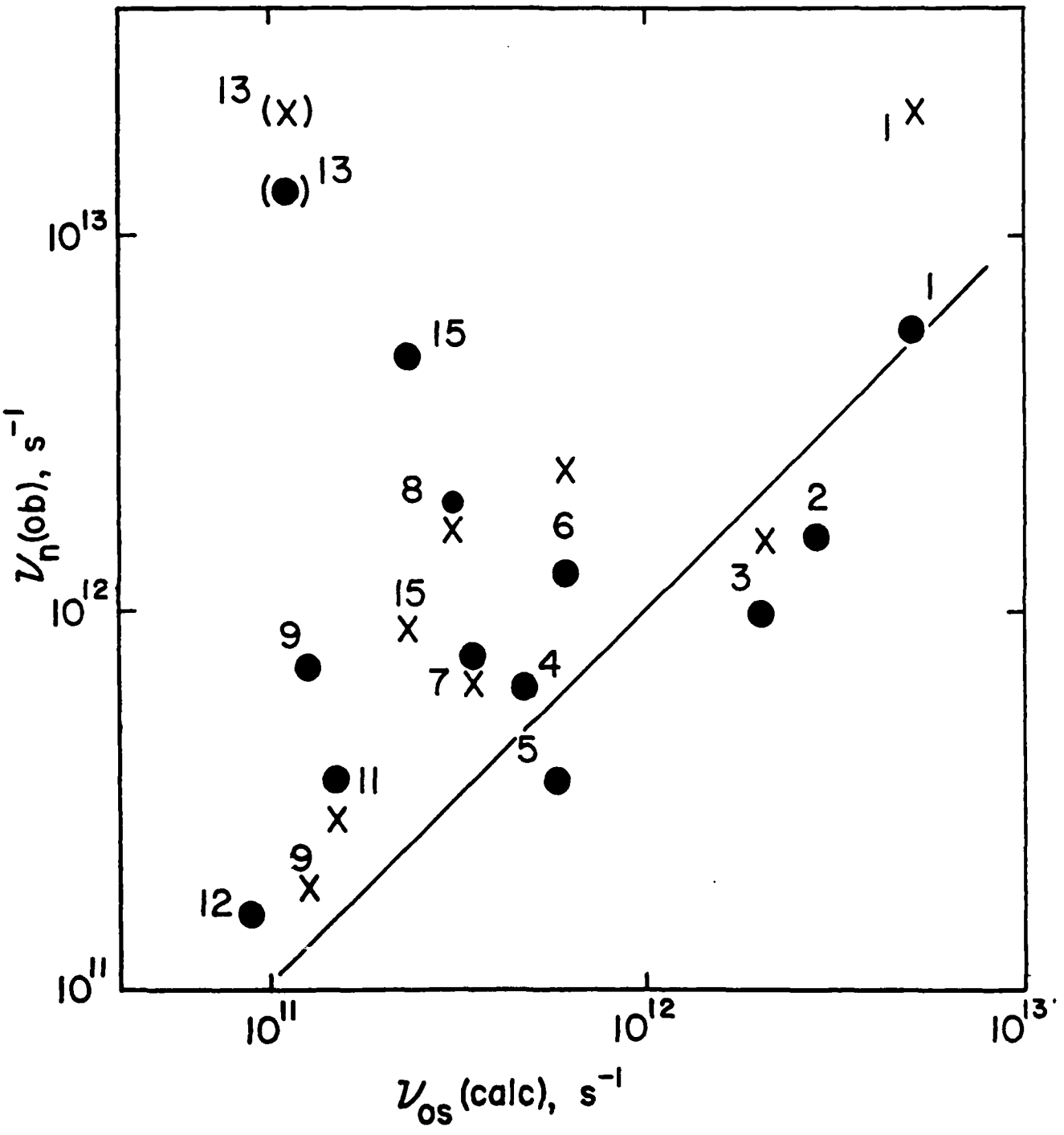

NIELSON ET AL

FIG 1

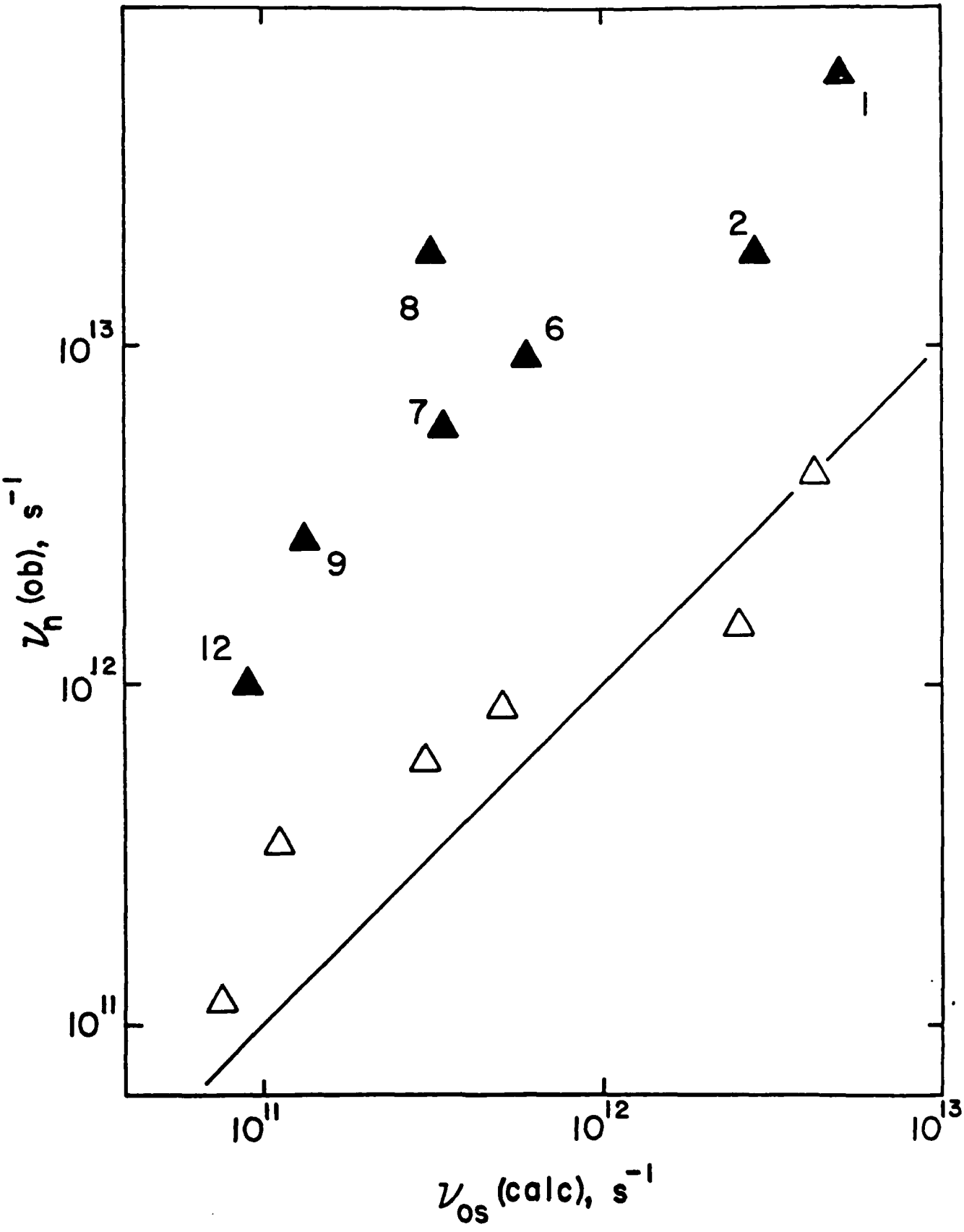

NIELSON ET AL

FIG 2

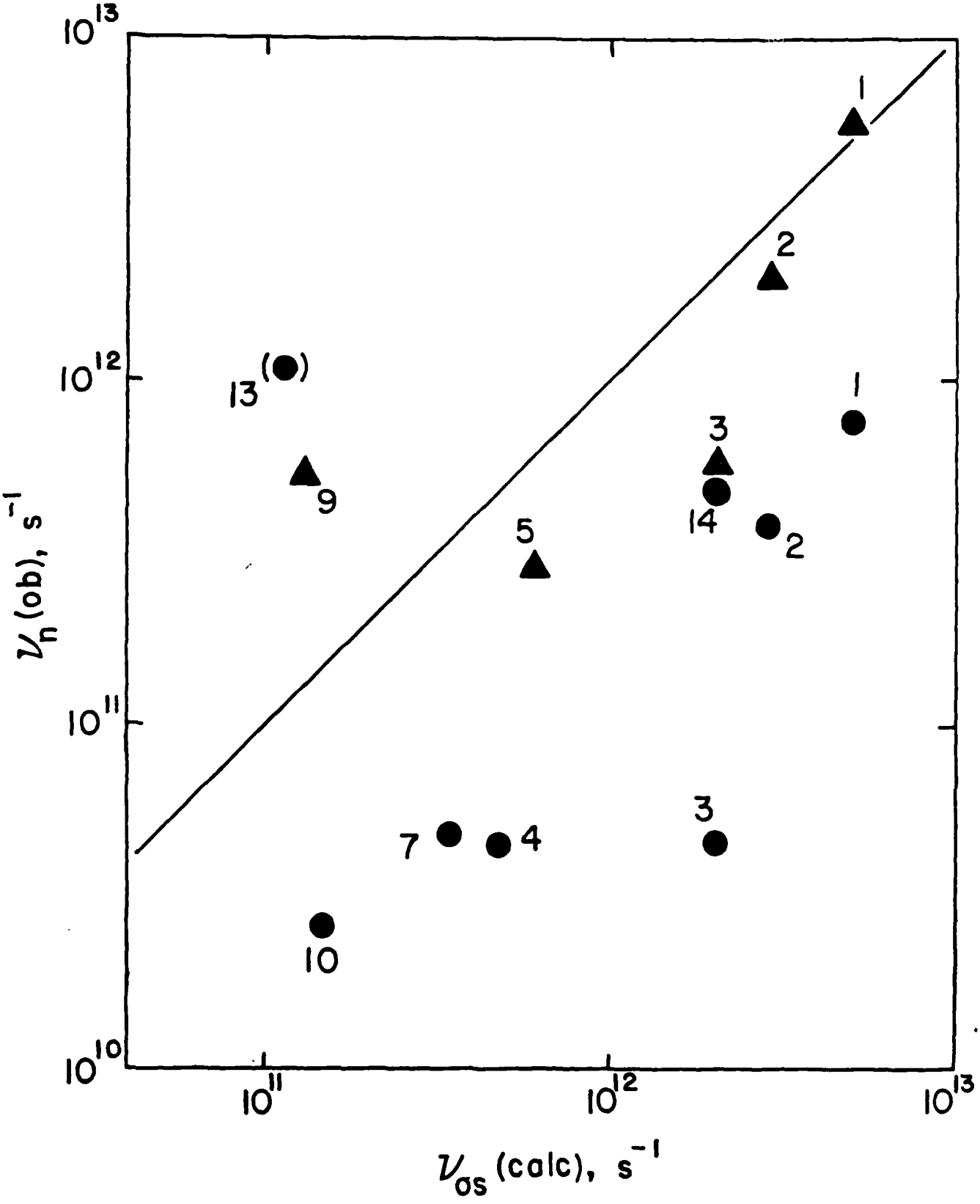

NIELSEN ET AL

FIG 3

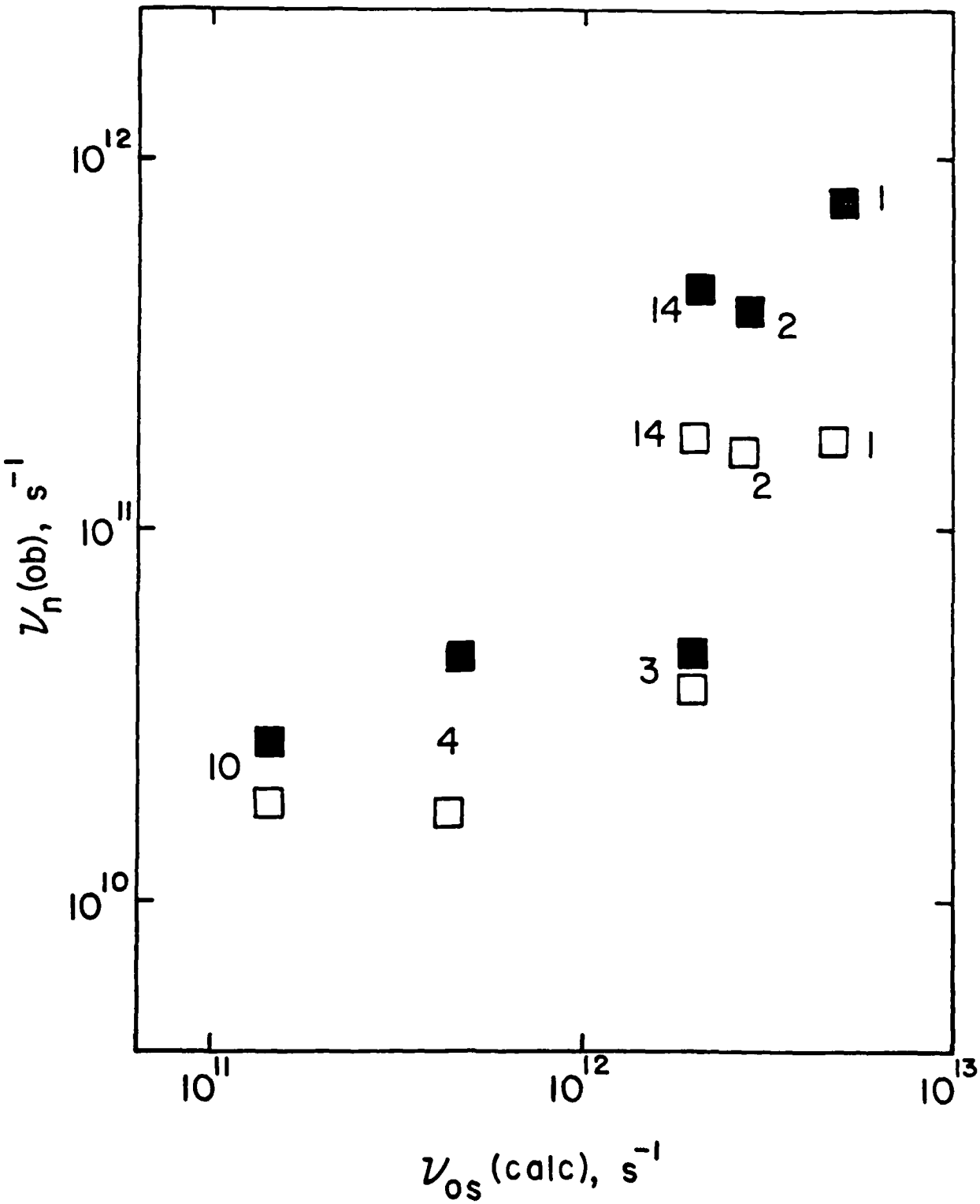

NIELSEN ET AL

FIG 4

SUPPLEMENTARY MATERIAL

TABLE A.1 ^1H nmr Parameters and Related Data for $Cp_2Co^{+/o}$ Self-Exchange at 200.07 MHz.

Solvent[a]	W_{DP}[b]	W_P[b]	ν_{DP}[b]	ν_D[b]	ν_P[b]	$[Cp_2CoBF_4]$[b]	$[Cp_2Co]$[b]	$[Et_4NBF_4]$[b]	T[b]	$k_{ex} \times 10^{-7}$[b]
AC-d_6	452	117	-9.31	5.93	-50.26	27.3	10.2	101	297	2.00
AC	187	117	-5.67	5.93	-50.26	73.2	19.0	102	297	1.74
AC	573	142	-8.32	5.94	-56.10	45.8	13.6	101	273	1.07
AC-d_6	406	127	-7.67	5.94	-53.34	45.8	13.6	101	283	1.40
AC-d^6	330	115	-7.38	5.94	-51.26	45.8	13.9	101	292	1.63
AC-d_6	33	117	-6.78	5.94	-49.20	45.8	13.7	101	302	2.93
AC-d_6	172	109	-6.49	5.94	-47.70	45.8	13.8	101	311	2.97
AC-d_6	145	105	-6.10	5.94	-46.01	45.8	13.8	101	320	3.39
AC-d_6	960	80	-1.70	5.93	-50.26	34.6	4.5	0	298	2.4
ACN	223	111	-9.98	5.67	-50.14	30.6	11.9	100	297	3.90
ACN	133	116	-7.97	5.67	-50.36	59.2	19.0	100	297	3.58
ACN-d_3	193	119	-6.35	5.67	-50.45	32.2	8.8	104	297	3.91
ACN	149	117	-8.40	5.67	-50.40	41.7	14.0	0	297	4.51
ACN	136	117	-4.66	5.67	-50.40	53.0	12.0	499	297	3.23
ACN-d_3	9.8	117	4.89	5.67	-50.40	89.8	1.3	103	297	3.10
ACN-d_3	196	123	-5.74	5.67	-53.07	48.9	11.8	98.8	283	2.61
ACN-d_3	147	112	-5.41	5.67	-51.24	48.9	11.8	98.8	292	3.38
ACN-d_3	119	110	-5.06	5.67	-49.48	48.9	11.8	98.8	302	4.10
ACN-d_3	94	105	-4.76	5.67	-47.86	48.9	11.8	98.8	311	5.12
ACN-d_3	75	104	-4.45	5.67	-46.31	48.9	11.8	98.8	320	6.52
ACN-d_3	167	112	-9.29	5.67	-50.77	45.5	16.4	0	295	3.69
ACN-d_3	131	108	-8.83	5.67	-49.11	45.5	16.4	0	304	4.67
ACN-d_3	104	105	-8.39	5.67	-47.54	45.5	16.3	0	313	5.85
ACN-d_3	85	104	-7.90	5.67	-46.27	45.5	16.1	0	321	7.44
ACN-d_3	72	103	-7.45	5.67	-44.72	45.5	16.0	0	331	8.98
ACN-d_3	145	111	-8.85	5.67	-50.03	45.5	16.0	0	299	4.24
ACN-d_3	440	112	-7.05	5.67	-50.77	12.9	3.8	0	295	4.05
ACN-d_3	347	108	-6.67	5.67	-49.11	12.9	3.8	0	304	5.08
ACN-d_3	256	105	-6.23	5.67	-47.54	12.9	3.7	0	313	6.43
ACN-d_3	204	104	-5.80	5.67	-46.04	12.9	3.7	0	323	7.78

ACN-d_3	158	103	-5.28	5.67	-44.72	12.9	3.6	0	331	9.76
ACN-d_3	370	111	-6.33	5.67	-49.88	12.9	3.6	0	300	4.63
PhCN	155	133	-12.27	5.72	-50.38	30.6	14.5	99.8	297	6.84
PhCN	127	133	-8.57	5.72	-50.38	45.0	15.4	104	297	5.42
PhCN	161	165	-3.44	5.68	-53.74	53.9	9.8	98.7	277	2.69
PhCN	123	151	-3.25	5.70	-52.27	53.9	9.8	98.7	284	3.49
PhCN	92	149	-2.88	5.72	-49.92	53.9	9.9	98.7	296	4.66
PhCN	54	128	-2.36	5.72	-46.43	53.9	9.9	98.7	316	8.42
PhCN	66	134	-2.62	5.72	-48.12	53.9	9.9	98.7	306	6.70
PhCN	46	122	-2.08	5.72	-44.45	53.9	9.9	98.7	329	10.2
PhCN	37	117	-1.89	5.72	-43.05	53.9	10.0	98.7	339	13.7
EC	73	109	-5.19	5.71	-49.02	68.3	17.0	sat. -90	297	5.61
EC	69	109	-3.25	5.71	-49.02	44.1	8.6	sat. -90	297	7.76
EC	81	109	-5.61	5.71	-49.02	62.3	16.2	sat. -90	297	5.47
EC	138	119	-12.26	5.71	-49.73	18.4	8.8	sat. -90	297	12.6
EC	153	119	-12.52	5.71	-49.73	21.7	10.6	sat. -90	297	9.32
EC	112	119	-11.10	5.71	-49.73	20.8	9.1	0	297	14.5
MC	121	128	-8.75	5.76	-48.42	30.6	11.2	99.3	297	8.07
MC-d_2	81	116	-5.65	5.76	-50.35	32.9	8.4	98.1	297	9.75
MC	28	116	1.74	5.76	-48.42	40.9	3.3	0	297	12.3
MC	101	116	-9.14	5.76	-48.42	45.6	17.3	286	297	6.82
MC-d_2	286	202	-1.85	5.76	-62.88	33.6	4.2	99.1	241	2.35
MC-d_2	200	171	-1.46	5.76	-59.37	33.6	4.2	99.1	253	3.09
MC-d_2	104	139	-.85	5.76	-53.58	33.6	4.2	99.1	278	5.29
MC-d_2	83	130	-.51	5.76	-51.95	33.6	4.1	99.1	284	6.35
MC-d_2	63	126	-.27	5.76	-49.98	33.6	4.1	99.1	294	8.25
MC-d_2	60	129	-.15	5.76	-49.24	33.6	4.0	99.1	297	8.56
DMF -	275	122	-8.11	5.93	-50.36	31.0	10.3	100	297	2.96
DMF	196	122	-4.73	5.95	-50.36	47.8	11.2	99.0	297	2.41
DMF	215	122	-3.32	5.95	-50.36	40.6	8.0	101	297	2.32
DMSO	128	153	-2.50	5.85	-49.73	61.3	10.8	100	297	2.63

DMSO-d_6	240	152	-3.04	5.85	-49.90	37.7	7.1	98.1	297	2.18
DMSO-d_6	280	167	-8.39	5.85	-50.72	47.7	16.1	101	292	2.01
DMSO-d_6	206	147	-7.97	5.85	-48.76	47.7	16.2	101	302	2.64
DMSO-d_6	166	149	-7.57	5.84	-47.34	47.7	16.1	101	311	3.31
DMSO-d_6	129	130	-7.16	5.85	-45.63	47.7	16.2	101	321	4.15
DMSO-d_6	105	123	-6.76	5.85	-44.23	47.7	16.1	101	330	5.10
DMSO-d_6	85	121	-6.65	5.85	-42.78	47.7	16.5	101	340	6.65
DMSO-d_6	702	280	-3.01	5.85	-50.21	13.8	2.6	0	295	1.95
DMSO-d_6	528	206	-2.86	5.85	-48.60	13.8	2.6	0	304	2.47
DMSO-d_6	389	166	-2.62	5.85	-46.91	13.8	2.6	0	313	3.19
DMSO-d_6	304	129	-2.38	5.85	-45.37	13.8	2.6	0	323	3.84
DMSO-d_6	240	105	-2.03	5.85	-44.03	13.8	2.6	0	331	4.55
DMSO-d_6	622	268	-2.63	5.85	-49.34	13.8	2.5	0	300	2.11
EtOH-d_6	850	132	-23.73	5.84	-48.25	2.5	10.9	99.9	298	3.5
EtOH-d_6	560	132	-18.50	5.84	-48.25	2.8	6.3	0	298	8.0
EtOH-d_6	300	132	-42.19	5.84	-48.25	2.8	21.3	101	298	3.2
HMPA	74	146	5.31	6.05	-50.72	53.8	0.71	97.4	297	0.540
HMPA	46	146	5.04	6.05	-50.72	123	2.2	101	297	0.534
HMPA	109	142	4.77	6.06	-50.01	51.5	1.2	99.5	300	0.643
HMPA	62	123	4.80	6.04	-46.57	51.5	1.2	99.5	321	1.04
HMPA	35	118	4.85	6.03	-43.71	51.5	1.2	99.5	339	1.77
HMPA	43	123	4.82	6.03	-45.25	51.5	1.2	99.5	329	1.49
MeOH	71	126	-2.81	5.81	-48.30	46.8	8.9	98.7	297	7.02
MeOH	72	126	-3.96	5.81	-48.30	50.6	11.2	98.5	297	7.29
MeOH[c]	281	86	-5.19	5.81	-49.52	53.6	13.3	98.5	299	7.68
MeOH[c]	188	85	-4.59	5.81	-46.71	53.6	13.2	98.5	315	10.7
MeOH[c]	123	76	-4.07	5.81	-44.19	53.6	13.2	98.5	326	15.3
MeOH[c]	310	92	-5.34	5.81	-50.49	53.6	13.2	98.5	293	7.17
MeOH[c]	362	107	-5.44	5.81	-51.34	53.6	13.1	98.5	288	6.31
NMF	99	147	-5.52	5.96	-48.22	39.0	10.5	99.3	297	7.39
NMF	98	147	-3.37	5.96	-48.22	40.5	8.4	100	297	5.9
PC	107	162	-1.65	5.77	-48.98	67.2	10.5	101	297	2.70
PC	177	162	-9.54	5.77	-48.98	54.0	21.0	105	297	3.10

Py	90	131	-2.06	5.71	-50.33	58.0	9.3	98.6	297	3.97
Py	128	131	-3.87	5.71	-50.33	40.0	8.3	100	297	4.45
Py	137	131	-7.81	5.72	-50.33	41.1	13.1	100	297	5.13
Py	102	138	-7.78	5.72	-49.88	43.3	13.9	0	297	7.38
Py	127	138	-6.90	5.72	-49.88	42.4	12.4	99.6	299	5.24
Py	218	144	-7.63	5.72	-53.80	42.4	12.3	99.6	279	3.07
Py	167	141	-7.18	5.72	-52.00	42.4	12.2	99.6	289	3.95
Py	115	131	-6.36	5.72	-48.51	42.4	12.2	99.6	308	5.52
Py	86	121	-5.98	5.72	-46.82	42.4	12.2	99.6	317	7.56
Py	77	123	-5.68	5.72	-45.40	42.4	12.2	99.6	327	8.55
Py	124	128	-6.51	5.72	-49.31	42.4	12.2	99.6	304	5.10
TMU	535	131	-7.91	5.99	-49.85	39.9	13.2	101	297	1.10
TMU	420	131	-7.77	5.99	-49.85	41.4	13.5	100	297	1.37

a) Solvent abbreviations are as follows: AC, acetone; ACN, acetonitrile; PhCN, benzonitrile; EC, 1,2-dichloroethane; MC, methylene chloride; DMF, dimethylformamide; DMSO, dimethylsulfoxide; HMPA, hexamethylphosphoramide; MeOH, methanol; NMF, N-methylformamide; PC, propylene carbonate; Py, pyridine; TMU, tetramethylurea.

b) Units are hertz for line widths, ppm for shifts, mM for concentrations, K for temperatures, and M^{-1} s^{-1} for rate constants. The value of W_D was 1 Hz.

c) The NMR data was collected at 469.58 MHz for these values.

TABLE A.2 ^1H NMR Parameters and Concentration Data for $Cp'_2Co^{+/o}$ Self-Exchange at 469.58 MHz.[a]

Solvent	W_{DP}	W_P	ν_{DP}	ν_D	ν_P	$[Cp'_2CoPF_6]$	$[Cp'_2Co]$	$[Et_4NBF_4]$	T	k x 10^{-8}
AC	254	45	14.78	1.83	45.46	13.6	5.7	99.7	298	2.38
AC	218	45	9.36	1.83	45.46	14.1	3.2	99.4	298	2.11
AC	457	60	10.71	1.83	50.03	14.1	3.2	99.4	271	1.26
AC	291	49	9.98	1.83	46.93	14.1	3.1	99.4	288	1.73
AC	197	45	9.23	1.83	44.92	14.1	2.9	99.4	305	2.29
AC	140	43	8.35	1.83	42.10	14.1	2.7	99.4	320	2.75
AC	102	42	7.80	1.83	40.66	14.1	2.6	99.4	330	3.44
ACN-d_3[b]	17.8	56	7.58	1.70	44.74	23.8	3.8	0	298	4.29
ACN	176	45	13.50	1.70	44.25	10.3	4.0	98.8	298	4.34
PhCN	172	49	14.06	1.54	45.50	20.3	8.1	99.9	298	2.44
DMF	131	50	6.49	1.79	45.50	18.1	2.2	99.3	298	2.01
DMSO-d_6[b]	12.9	71	3.30	1.68	45.00	21.8	0.8	0	298	1.62
DMSO	201	59	6.79	1.68	45.50	12.2	1.6	0	298	2.05
HMPA	564	55	6.00	1.83	45.58	21.4	2.3	101	298	0.35
PC	217	61	9.11	1.73	45.50	10.8	2.2	0	298	2.78

a) Solvent abbreviations and units are the same as Table A.1. The value of W_D was 1 Hz.

b) The NMR data was collected at 200.07 MHz for these values.

TABLE A.3 ^1H NMR Parameters and Concentration Data for $Cp'_2Fe^{+/o}$ Self-Exchange at 469.58 MHz.[a]

Solvent	W_{DP}	W_P	ν_{DP}	ν_D	ν_P	$[Cp'_2Fe]$	$[Cp'_2FeBF_4]$	$[Et_4NBF_4]$	T	$k_{ex} \times 10^{-7}$
PhCN	427	372	-4.47	1.51	-37.11	24.9	4.6	0	298	4.98
Py	579	442	-6.43	1.65	-36.60	28.1	7.5	0	298	3.91

a) Solvent abbreviations and units are the same as Table A.1. The value of W_D was 1 Hz.

OFFICE OF NAVAL RESEARCH

Contract N00014-86-K-0556

Technical Report No. 77

Solvent Dynamical Effects in Electron Transfer: Comparisons of Self-Exchange Kinetics for Cobaltocenium-Cobaltocene and Related Redox Couples with Theoretical Predictions

by

R. M. Nielson, G. E. McManis, M. N. Golovin, and M. J. Weaver

Prepared for Publication

in the

Journal of Physical Chemistry

Purdue University

Department of Chemistry

West Lafayette, Indiana 47907

February 17, 1988

END

DATE

FILMED

5-88

DTIC